

NASA TECHNICAL
MEMORANDUM

NASA TM X-73,101

NASA TM X-73,101

A METHOD FOR GENERATING NUMERICAL PILOT OPINION RATINGS
USING THE OPTIMAL PILOT MODEL

Ronald A. Hess

Ames Research Center
Moffett Field, Calif. 94035

(NASA-TM-X-73101) A METHOD FOR GENERATING
NUMERICAL PILOT OPINION RATINGS USING THE
OPTIMAL PILOT MODEL (NASA) 58 p HC \$4.50

N76-21217

CSSL 05H

Unclas

G3/08 25155

February 1976



1. Report No. TM X-73,101	2. Government Accession No.	3. Recipient's Catalog No.	
4. Title and Subtitle A METHOD FOR GENERATING NUMERICAL PILOT OPINION RATINGS USING THE OPTIMAL PILOT MODEL		5. Report Date	
		6. Performing Organization Code	
7. Author(s) Ronald A. Hess*		8. Performing Organization Report No. A-6427	
		10. Work Unit No. 513-54-01	
9. Performing Organization Name and Address Ames Research Center Moffett Field, Calif. 94035		11. Contract or Grant No.	
		13. Type of Report and Period Covered Technical Memorandum	
12. Sponsoring Agency Name and Address National Aeronautics and Space Administration Washington, D.C. 20546		14. Sponsoring Agency Code	
		15. Supplementary Notes *On assignment from Naval Postgraduate School, Monterey, Calif.	
16. Abstract A method for generating numerical pilot opinion ratings using the optimal pilot model is introduced. The method is contained in a rating hypothesis which states that the numerical rating which a human pilot assigns to a specific vehicle and task can be directly related to the numerical value of the index of performance resulting from the optimal pilot modeling procedure as applied to that vehicle and task. The hypothesis is tested using the data from four piloted simulations. The results indicate that the hypothesis is reasonable, but that the predictive capability of the method is a strong function of the accuracy of the pilot model itself. This accuracy is, in turn, dependent upon the parameters which define the optimal modeling problem. A procedure for specifying the parameters for the optimal pilot model in the absence of experimental data is suggested.			
17. Key Words (Suggested by Author(s)) Optimal pilot models Handling qualities Pilot ratings Man-machine performance		18. Distribution Statement Unlimited STAR Category - 08	
19. Security Classif. (of this report) Unclassified	20. Security Classif. (of this page) Unclassified	21. No. of Pages 58	22. Price* \$4.25

TABLE OF CONTENTS

	<u>Page</u>
INTRODUCTION	1
Background.	1
Rating Hypothesis	2
Testing the Hypothesis.	3
RATING FUNCTION.	4
Data Base	4
Optimal Pilot Modeling.	5
Modeling Results.	7
Discussion.	8
EXAMPLE 1. UH-1H HOVER.	10
Vehicle/Task Description.	10
Optimal Pilot Modeling.	10
Modeling Results.	13
Discussion.	14
EXAMPLE 2. UH-1H LANDING APPROACH	14
Vehicle/Task Description.	14
Optimal Pilot Modeling.	16
Modeling Results.	17
Discussion.	18
EXAMPLE 3. H-19 HOVER	19
Vehicle/Task Description.	19
Optimal Pilot Modeling.	19
Modeling Results.	20
Discussion.	20
CONCLUSIONS AND RECOMMENDATIONS.	21
REFERENCES	22
TABLES	24
FIGURES.	41

A METHOD FOR GENERATING NUMERICAL PILOT OPINION RATINGS
USING THE OPTIMAL PILOT MODEL

Ronald A. Hess*

Ames Research Center

INTRODUCTION

Background

The optimal-control model of the human operator has been shown to be a useful tool in the analysis of pilot-vehicle systems [1-3]. The model has been used in a variety of research efforts and has demonstrated a capability of generating estimates of pilot performance ranging from simple root-mean-square (RMS) tracking performance to instrument scanning behavior. Model-based measures of workload have also been proposed and utilized [4,5]. This report summarizes a research effort aimed at empirically extending the capabilities of the optimal pilot model to allow the generation of numerical handling qualities ratings utilizing the Cooper and Cooper-Harper rating scales [6,7]. Since numerical pilot ratings constitute the ultimate evaluation of any new aircraft, a pilot model which generates such ratings is particularly desirable.

The concept of generating pilot ratings using analytical pilot models is not new. Most previous studies, however, e.g. [8-10], have centered upon the classical frequency domain pilot representations as discussed in [11], whereas this study utilizes the state-space optimal control model. Since the optimal pilot model is finding increased utilization in man-machine system analysis, a rating generation capability would be quite useful.

A detailed description of the optimal pilot model, itself, is beyond the scope of this report. The reader is instead referred to [1] for specifics. However, the basic hypothesis behind the model can be given as follows:

Subject to his inherent limitations, the well trained, well motivated pilot, behaves in an optimal manner. The pilot's control characteristics can be modeled by the solution of an optimal linear control and estimation problem, with certain specifications. As utilized in this study, these specifications can be summarized as follows:

(1) Time Delay - A pure time delay is included in each of the pilot's control outputs.

(2) Neuromuscular Dynamics - Each output neuromuscular system is modeled as a first-order lag, or equivalently, control rate appears in the quadratic index of performance.

*On assignment from Naval Postgraduate School, Monterey, Calif.

(3) Observation and Motor Noise - Each variable which the pilot observes from his display is assumed to contain pilot-induced additive white noise which scales with the variance of the observed variable. Each control output is assumed to contain pilot-induced additive white noise which scales with the variance of the control.

(4) Rate Perception - If a variable is displayed explicitly, the pilot also perceives the first derivative of the variable but no higher derivatives. The first derivative of the displayed variable is also noise contaminated.

The placement of the pilot time delay at the control output constitutes the only major deviation from the model of Kleinman et al. Here, the delay is represented by a Pade' approximation and is treated as part of the plant dynamics. The model of [1] subsumes the delay into the observation process. The only advantage which the Pade' approximation affords is that it allows direct use of existing computational algorithms for the solution of optimal estimation and control problems.

In what follows, a "displayed" variable will refer to a variable explicitly displayed to the pilot by the position of a display indicator. A "perceived" variable will refer to the time rate of change of a displayed variable. An "observed" variable will refer to either a displayed or perceived variable. Figure 1 is a block diagram of a pilot-vehicle system.

Rating Hypothesis

Perhaps the most critical step in formulating the optimal pilot model lies in the selection of weighting matrices for the quadratic index of performance:

$$J = E \left\{ \lim_{T \rightarrow \infty} \frac{1}{T} \int_0^T [\underline{y}^T(t) \underline{Q} \underline{y}(t) + \underline{u}^T(t) \underline{R} \underline{u}(t)] dt \right\}$$

Here, $\underline{y}(t)$ represents a linear combination of system states, i.e.,

$$\underline{y}(t) = \underline{C}' \underline{x}(t)$$

In order to enhance the face value of the rating scheme to be described, the variables selected for inclusion in the vector $\underline{y}(t)$ need to be directly observable by the pilot. In this study, $\underline{u}(t)$ represents the pilot control motions before the time delay and neuromuscular dynamics are encountered in figure 1. It is assumed that $\underline{u}(t)$ is observable by the pilot in all cases. The selection of the elements of the \underline{Q} and \underline{R} matrices is not a trivial step. In this study, the elements of these diagonal matrices were selected on the basis of maximum "allowable" deviations of the variables included in $\underline{y}(t)$ and $\underline{u}(t)$. Such a selection scheme is suggested in [12] for optimal control problems in general and utilized in [4] for the optimal model.

The pilot rating hypothesis to be investigated can be stated as follows:

IF

- (1) the index of performance and model parameters in the optimal pilot modeling procedure yield a dynamically representative model of the human pilot,
- (2) the variables selected for inclusion in the index of performance are directly observable by the pilot,
- (3) the weighting coefficients in the index of performance are chosen as the squares of the reciprocals of maximum "allowable" deviations of the respective variables, and these deviations are consonant with the task as perceived by the pilot,

THEN

The numerical value of the index of performance resulting from the modeling procedure can be related to the numerical pilot rating which the pilot assigns to the vehicle and task by

$$R = R(J)_s$$

where $R(J)_s$ represents a monotonic function of the value of the index of performance J . The subscript 's' denotes the particular rating scale being utilized by the pilot.

Implicit in the hypothesis is the assumption that once the function $R(J)_s$ has been found for a specific scale 's', it can be utilized to assign pilot ratings to any vehicle and task, provided, of course, that the assumptions (1)-(3) are met.

The possibility that a correlation exists between pilot performance and pilot ratings has been indicated in the literature. McDonnell demonstrates this in an experimental study using simple controlled elements [13] and Téper in adapting a rating functional for "Paper Pilot" using VTOL aircraft dynamics [14]. The idea that a single rating function is applicable to any task is not unreasonable in view of the manner in which the index of performance is defined. First, the index contains only variables observable by the pilot and further, only variables whose deviations are considered pertinent to the task. Second, these variables are normalized with respect to maximum allowable deviations where these allowable deviations are consonant with the vehicle and task as perceived by the pilot.

Testing the Hypothesis

The analytical study which follows does not constitute a proof of the preceding hypothesis. Indeed, the empirical nature of the analysis precludes such a proof. Rather, the hypothesis was tested in the following manner:

First, the data from a well documented experimental study, [13], was used with optimal pilot modeling results to ascertain whether a rating function $R(J)_s$ exists for a single-axis compensatory tracking task, employing a single controller and display element.

Second, the data from an experiment involving a more complex task (longitudinal helicopter hover), two controllers (longitudinal cyclic and collective) and an integrated cathode-ray-tube (CRT) display with several elements was used along with modeling results to compare model generated ratings with pilot generated ratings.

Third, the ability of the rating scheme to assign a general flying quality level, as per [15] was investigated using the data from another complex task (longitudinal helicopter landing approach), two controllers (longitudinal cyclic and collective) and a CRT display.

Finally the data from the simulation of another helicopter in hover [14] with a single controller (longitudinal cyclic) and a CRT display, was utilized to compare pilot and model generated handling qualities ratings.

In each of these cases, the primary difficulty in applying the rating hypothesis was in determining whether a dynamically representative model of the human pilot had been obtained. Determining the validity of any pilot model usually involves comparing characteristics of model generated closed-loop signals with those from piloted simulation. The signal characteristics used in any comparison can be ranked in terms of the information they convey about the signals themselves. For example, the average power in a signal conveys less information about the signal than does its power spectral density, which, in turn conveys less information than the signal time history itself. Thus, a pilot model whose validity was based upon comparisons of model generated and experimental mean square signal values would inspire less confidence than a model whose validity rested upon describing function comparisons (essentially obtained from power and cross power spectral densities). In turn, the latter model would defer to one whose validity rested upon a direct comparison of signal time histories.

Experimental pilot describing function data was obtained in only the first of the simulation studies mentioned above. Thus, the validity of the pilot models to be developed for the helicopter approach and hover tasks will rest upon favorable comparison of model generated and experimental RMS tracking scores.

RATING FUNCTION

Data Base

The data for the first part of this study was taken from [13], a well documented investigation of pilot rating techniques. Mean square error scores, pilot describing functions and various numerical pilot ratings were collected for a variety of simple controlled elements in compensatory, single-axis

laboratory tracking tasks. Figure 2 is a block diagram representation of this task. Note that the primary task is single-axis in nature. The secondary task was included to measure excess control capacity with a cross-adaptive algorithm and was not utilized in the tracking runs pertinent to this study. The commanded input θ_c was obtained as the sum of sinusoids. The amplitudes and frequencies of the particular input pertinent to this study are shown in table 1. The primary task was represented as a longitudinal tail-chase condition for a gunnery run in air combat. The lead aircraft was taking evasive action. The seven primary task controlled elements pertinent to this study are shown in table 2. These seven elements were chosen since the associated pilot ratings spanned the ranges of the rating scales of interest.

A fixed base simulator was utilized with a CRT display and fighter-aircraft type center-stick. The display is shown in figure 3 with the lead aircraft's wings represented by the moving line. An analog computer generated the controlled element dynamics. The eye-to-display distance was about 46 cm. A total of forty-four configurations (a configuration consisting of a specific controlled element and input) were presented to the pilots in a random sequence. As indicated previously, only the data of seven of the configurations were of interest here. For each configuration, the pilot had to perform two sequential tasks, only the first of which is pertinent to this study. For the first task, he was asked to track longitudinally to minimize the pitch error. During this 120 sec period, the secondary task was inoperative and the pilot was asked to formulate his opinion of the configuration based on the task performance criterion stated as follows:

"Best gunnery results will probably be obtained if error is kept less than .75 cm."

Approximately 15 sec were allowed before each run for the subject to reach steady-state tracking so that the first 100 sec portion of the 120 sec run would be suitable for describing function computations and performance measures. At the completion of the 120 sec run, the pilot was asked to write down the ratings on a clipboard. Two of the scales which he utilized are shown in tables 3 and 4. The second task was two-axis in nature and will not be discussed here. Two pilots participated in the experiments. Since describing function results for only one of the pilots were published, only the data for that subject was used in the modeling to be described.

Optimal Pilot Modeling

The equations which define the optimal pilot model follow:

system state equations

$$\dot{\underline{x}}(t) = \underline{A} \underline{x}(t) + \underline{B} \underline{u}(t) + \underline{\gamma} \underline{w}(t)$$

$$E[\underline{w}(t) \underline{w}^T(t + \sigma)] = \underline{F} \delta(\sigma)$$

REPRODUCIBILITY OF THE
ORIGINAL PAGE IS POOR

where $\underline{x}(t)$ represents the state, $\underline{u}(t)$ the pilot's control output before his time delay and neuromuscular dynamics are encountered and $\underline{w}(t)$ white noise disturbances to be described.

(1) The controlled element dynamics, are described in general as

$$Y_c(s) = \frac{K_B a}{s(s + b)}$$

where K_B , a and b are given in table 2. Note that the K_B/s dynamics are represented as $K_B(40)/s(s + 40)$ for computational simplicity. The additional first-order denominator with break frequency of 40 rad/sec is well beyond the bandwidth of interest for this study.

(2) The sinusoidal input was represented by white noise with unity covariance passed through an appropriate shaping filter. The filter was chosen such that the frequency distribution of its output power closely matched the frequency distribution of power of the sinusoidal input, θ_c . Figure 4 shows this matching. The filter transfer function is given by

$$G_1(s) = \frac{3.674}{s^2 + 3s + 2.25}$$

The necessity of using a second-order filter as opposed to one of first-order stems from the fact that a state variable corresponding to the time rate of change of the input was needed in defining one of the observed variables (error rate).

(3) The pilot's effective time delay was modeled by a second order Pade' approximation as

$$e^{-\tau s} = \frac{(s - 4/\tau)^2}{(s + 4/\tau)^2}$$

(4) The pilot's neuromuscular dynamics were modeled as a first order lag

$$G_2(s) = \frac{1}{T_N s + 1}$$

This is dynamically equivalent to including a weighting on control rate in the index of performance and adjusting the weighting coefficient on this term to yield a predetermined value of T_N [1]. In this study, the control rate term is not included in the index of performance, however.

(5) The motor noise, $\underline{v}_m(t)$ is white in nature with covariance

$$E[\underline{v}_m(t) \underline{v}_m^T(t + \sigma)] = \rho' \pi E[\underline{u}(t) \underline{u}^T(t + \sigma)] \delta(\sigma)$$

Here ρ' is the predetermined noise-signal ratio for the motor noise.

observation equations

$$z(t) = H x(t) + v(t)$$

$$E[w(t) w^T(t + \sigma)] = G \delta(\sigma)$$

where $H x(t)$ represents the vector of variables displayed to or perceived by the pilot and $v(t)$ the vector of observation noises. The covariance of the individual observation noises is given by

$$E[v_i(t) v_i(t + \sigma)] = \frac{\rho_i \pi E[z_i'(t) z_i'(t + \sigma)] \delta(\sigma)}{\hat{f}^2(z_i')}$$

where $z_i'(t) = H x_i(t)$ and ρ_i is the noise-signal ratio associated with the i^{th} observed variable and $\hat{f}(z_i')$ is the amplitude-dependent pure-gain Gaussian-input describing function for a threshold-type nonlinearity associated with the i^{th} observed variable [16]. This nonlinearity models pilot indifference thresholds on the observed variables [2]. Since there is only a single display indicator for the single-axis task, no task interference occurs and the model for task interference [4,17] need not be employed.

index of performance

$$J = E \left\{ \lim_{T \rightarrow \infty} \frac{1}{T} \int_0^T [y^T(t) Q y(t) + u^T(t) R u(t)] dt \right\}$$

where $y(t)$ is given by $y(t) = C x(t)$ and $u(t)$ is the pilot's output before his effective time delay and neuromuscular dynamics are encountered. Table 5 gives the general form of the matrices which constitute the problem definition.

Modeling Results

The pilot modeling to be described was aimed at analytic duplication of the tracking experiments described in [13]. Particular attention was paid to ensuring that the assumptions of the rating hypothesis were met:

(1) In an attempt to obtain a dynamically representative model of the human pilot, model parameters were selected so that a fair match existed between experimental and analytical RMS error scores. After the match was verified, the experimental and analytical describing functions were compared.

(2) The variables selected for inclusion in the index of performance were error, $\theta_e(t)$, and optimal control motion, $u(t)$, both observable by the pilot.

(3) The weighting coefficients in the index of performance were chosen as the squares of the reciprocals of the estimated maximum "allowable" deviations of the problem variables.

Table 6 presents the nominal (a-priori) pilot model parameters used in the study. As indicated in table 6, all problem variables are expressed in terms of equivalent display indicator movement in cm. For example, control stick movement of 1.0 cm refers to the control stick movement which would yield a display indicator movement of 1 cm with a controlled element $Y_c = 1.0 \text{ cm/cm}$ and $\theta_c(t) = 0$.

Table 7 lists the pilot model parameters that yielded the error scores of figure 5. This figure illustrates a comparison of RMS error scores from [13] and those from the modeling procedure. Figures 6-9 show four representative measured and model generated open-loop describing functions $Y_p Y_c(j\omega)$. Finally, figures 10 and 11 illustrate the rating functions $R(J)_s$ for the Cooper and Cooper-Harper rating scales.

Discussion

The values of τ , T_N , and ρ shown in table 6 were chosen on the basis of values found in [1] for similar tasks. The τ value was chosen somewhat smaller, 0.1 sec rather than the 0.15-0.18 sec in [1]. The noise-signal ratio ρ' , however, was selected considerably larger than the 0.003 value proposed in [1] since the experiments of [13] used a spring restrained control stick whereas the experiments in [1] used an ideal force manipulator. The nominal indifference thresholds of 0.5 cm and 0.5 cm/sec (0.63 deg and 0.63 deg/sec of visual arc) represent subjective estimates. These values are considerably larger than values normally associated with physiological thresholds, e.g., 0.05 deg and 0.05-0.1 deg/sec of visual arc.

The variables and weighting coefficients appearing in the index of performance represent subjective estimates of what constitute pertinent problem variables and maximum allowable deviations. The maximum allowable deviation on error was chosen as 1.0 cm, somewhat larger than the 0.75 cm, criterion value stated in the instructions to the pilot.

The rule of thumb used in adjusting the nominal pilot model parameters of table 6 to achieve a dynamically representative model of the human pilot was as follows:

Change as few of the nominal parameters as little as possible in order to achieve a satisfactory match between experimental and analytical RMS error scores. After doing this for all the controlled elements in question, compare the experimental and analytical open-loop describing functions. If a reasonable match is obtained in the describing function comparison, assume dynamically representative models of the pilot have been obtained.

As figure 5 indicates, the RMS error matching was quite good with the exception of the 10 Kp/s^2 point. Table 7 shows that, with the exception of the

0.1 K_B/s^2 task, the only nominal pilot model parameter which was altered was ρ' , the noise-signal ratio for the motor noise. In the 0.1 K_B/s^2 case, the indifference thresholds on error and error rate were increased to 2.0 cm and 2.0 cm/sec, respectively. The low value of the experimental RMS error for the 10 K_B/s^2 is suspect. In [13], the recorded normalized mean square error ($\bar{\theta}_e^2/\bar{\theta}_c^2$) for this run is an order of magnitude below that for an identical controlled element with $\sqrt{\bar{\theta}_c^2} = 0.5$ cm. The mean square error for $\sqrt{\bar{\theta}_c^2} = 1.5$ cm was not recorded, and the author assumes that this indicates saturation of the analog integrator providing $\bar{\theta}_e^2$, i.e., a normalized mean square error score even greater than that for the 0.5 cm input case. This incongruity led the author to ignore the RMS comparison for this case. The reduction of ρ' as the controlled elements become more difficult, i.e. as the non-zero pole in the controlled element moved toward the origin, is a reasonable parametric variation. This reduction corresponds to more precise control motion with increasing task difficulty.

The analytic increase in the indifference thresholds for the 0.1 K_B/s^2 case is, to some extent, corroborated by the fact that the experimentally determined "relative remnant" from [13] for this element is lowest of the seven elements studied here. The relative remnant is defined as the ratio of the amount of power in the control stick output which is linearly correlated with the system input to the total power in the control stick output. Thus, when the relative remnant is small, the pilot is introducing a considerable amount of "noise" either through nonlinearities (e.g., indifference thresholds) time variations, or direction noise injection. The relative remnants, denoted ρ_{ac}^2 are shown in figures 6-9 for the respective controlled elements. The ρ_{ac}^2 for the 0.1 K_B/s^2 is 0.387, and considerably smaller than those for the other tasks. No describing function comparison for this element was possible since the experimentally determined describing function from [13] was unreliable due to poor signal-to-noise ratios.

The describing function comparisons of figures 6-9 are generally good. The phase comparisons indicate that a larger effective time delay should have been utilized in the analysis, say on the order of 0.15 to 0.2 secs. For the purposes of this study, however, the predicted describing functions were considered acceptable.

The seven points in each of the rating curves of figures 10 and 11 were obtained by plotting the value of the index of performance, J, resulting from the modeling procedure versus the assigned pilot rating for each of the seven controlled elements under study. The curves are similar, but not identical in shape. Thus, it does appear that rating functions of the form $R(J)_s$ exist for single-axis compensatory tracking tasks employing a single controller and display element. The object of the following sections is to ascertain whether the curves can be used to generate ratings and handling qualities levels for more complex tasks.

EXAMPLE 1. UH-1H HOVER

Vehicle/Task Description

This task involved the simulated longitudinal control of a UH-1H unaugmented helicopter in hover, in the presence of longitudinal turbulence. The pilot's task involves keeping the vehicle over the center of a square landing pad 15.2 m (50 ft) on a side. The pilot must also keep the vehicle at a prescribed height above the ground. The value of this datum height is immaterial in this analysis, save that the vehicle is not in ground effect. The pilot has two controls, the longitudinal cyclic and the collective pitch.

The fixed base pilot-in-the-loop simulation of the longitudinal task was conducted on the Naval Postgraduate School's hybrid computer. The vehicle dynamics were simulated on the analog computer, the displays were generated on a stroke-written CRT graphics terminal with the digital computer driving the display elements. Table 8 lists the vehicle aerodynamic data. Table 9 shows the turbulence spectrum. Figure 12 shows the display format. In the "baseline" configuration, the flight director bar was omitted. In the "director" configuration, it was included. The director signal was synthesized using the methods of [18] and will not be discussed here. The nominal eye-to-display distance was 0.762 m (2.5 ft). The cyclic control device was a spring-restrained aircraft-type center stick with a force-displacement gradient of 3.50 newtons/cm (2 lb/in.). The collective control was a device restrained only with an adjustable friction brake set to give a breakout force of 2.22 newtons (0.5 lbs).

A single well trained UH-1 pilot was utilized in the experiment. After considerable training, twenty data runs were taken, each of 90 sec duration, using the baseline and director displays. The displays were presented in alternate fashion, five runs with the baseline, then five with the director, etc. The performance measures recorded were RMS measures of longitudinal displacement from the pad center, x , longitudinal groundspeed, \dot{x} , pitch attitude, θ , time rate of change of pitch attitude, $\dot{\theta}$, altitude deviation from the nominal, h , altitude rate, \dot{h} , cyclic control motion, δ_B , and collective control motion, δ_C . In addition, pilot opinion ratings were elicited using the Cooper-Harper scale of table 4.

Optimal Pilot Modeling

With three exceptions, the general form of the optimal pilot model for the hover is identical to the form of the model used to obtain the rating functions. These exceptions are:

(1) The pilot's effective time delay was modeled by a first order Pade' approximation:

$$e^{-\tau s} = \frac{(s - 2/\tau)}{(s + 2/\tau)}$$

(2) The motor noise for the collective control contains a residual term which does not scale with the variance of the control motion, $u_2(t)$,

$$v_{m_2}^1(t) = v_{m_2}(t) + r(t)$$

where $v_{m_2}(t)$ is the white motor noise whose intensity scales with the variance of $u_2(t)$ and $r(t)$ is the residual white noise term.

(3) Task interference was considered in selecting the noise-signal ratios, ρ_i , for the observed variables.

The reduction in the order of the Pade' approximation was done to reduce the total number of state variables for computational efficiency. The necessity of including residual motor noise on the collective was based upon the unrealistically small collective motion and vehicle vertical motion which resulted in the modeling procedure when this noise was not included. In retrospect, such behavior should have been expected. With the horizontal turbulence primarily exciting the vehicle's horizontal translation and pitch attitude mode, the optimal control policy for the collective was essentially to keep the device at its still-air trim position. In reality, however, this trim position is never known precisely by the pilot. Off-nominal collective position excites the vertical translation mode of the helicopter which the pilot then corrects with further collective motion, etc. To model this trim uncertainty, the residual noise was added to the control $u_2(t)$ (the pilot's collective motion before his time delay and neuromuscular dynamics are encountered). The covariance of the residual noise was set to 1.0 cm^2 , where here the cm units refer to control motion measured at the pilot's hand. This value was chosen by assuming that the pilot has an average uncertainty ($\pm 1\sigma$ value) of $\pm 1.0 \text{ cm}$ in collective trim position for the baseline. For the director configuration, a value of $\pm 0.75 \text{ cm}$ was found to yield better RMS performance.

In contrast to the situation in which the pilot need only concern himself with a single task, e.g., control of an aircraft's pitch attitude, task interference implies the pilot tracking behavior and performance which accompany shared attention, e.g., control of both pitch attitude and altitude deviations. The model for task interference does not imply pilot scanning behavior, however. Just as in [4], the effects of task interference were modeled as an increase in the nominal noise-signal ratios for each observed variable. Thus,

$$\rho_i = \rho \cdot \frac{1}{f_t} \cdot \frac{1}{f_s} \cdot \frac{1}{f_i}$$

where

ρ_i = noise-signal ratio associated with the i^{th} observed quantity when attention is being shared

ρ = noise-signal ratio associated with "full attention" to the i^{th} display

f_t = fraction of attention devoted to the control task as a whole

f_s = fraction of attention devoted to sub-task 's', e.g., longitudinal control

f_i = fraction of attention devoted to the i^{th} observed quantity in sub-task 's', e.g., control of pitch attitude in the longitudinal sub-task.

In the baseline configuration for the display of figure 12, there are three displayed quantities and three perceived quantities. The displayed quantities are:

(1) the longitudinal displacement of the helicopter from the center of the landing pad, x

(2) the pitch attitude, θ

(3) the altitude deviation of the helicopter from the datum, h .

The three perceived quantities are \dot{x} , $\dot{\theta}$, and \dot{h} , the time derivatives of the displayed quantities. No task interference is assumed to occur between displayed and perceived variables, only between displayed variables [17]. Thus, a displayed quantity and its time derivative have the same ρ_i .

In modeling for the hover task,

$$f_t = 1.0 \quad f_s = 1.0 \quad f_i = 0.333 \quad i = 1, 2, 3$$

Thus, the pilot is assumed to be devoting all his attention to the control task, all of the control task attention to the longitudinal task and 1/3 of the longitudinal task attention to each of the three displayed quantities. The f_t and f_s values are obvious choices in light of the simulation scenario. Normally, the f_i are chosen on the basis of a set which minimizes the index of performance, J , and which satisfies the constraints

$$\sum_{i=1}^n f_i = 1.0$$

$$f_i > 0. \quad i = 1, 2, \dots, n,$$

n = number of displayed quantities

Although an efficient algorithm for solving for the optimum f_i has recently been developed [19], it was assumed in this analysis that each of the three displayed quantities received equal attention. The performance comparison to be made indicates that this was not an unreasonable choice.

In the director configuration for the display of figure 12, it was assumed that there are two displayed quantities and two perceived quantities. The displayed quantities are:

(1) the cyclic director signal, δ_{B_D}

(2) the altitude deviation of the helicopter from the datum, h .

The two perceived quantities are $\dot{\delta}_{B_D}$ and \dot{h} , the time derivatives of the displayed quantities. Here

$$f_t = 1.0 \quad f_s = 1.0 \quad f_i = 0.5 \quad i = 1,2$$

Here, the pilot is assumed to devote all of his attention to the control task, all of the control task attention to the longitudinal task and 1/2 of the longitudinal task attention to each of the displayed quantities, δ_{B_D} and h .

Modeling Results

The pilot modeling was aimed at analytic duplication of the tracking experiments for the UH-1H hover. Again, attention was paid to ensuring that the assumptions of the rating hypothesis were met:

(1) In an attempt to obtain a dynamically representative model of the human pilot, model parameters were selected so that a fair match existed between experimental and analytical RMS error scores.

(2) The problem variables selected for inclusion in the index of performance were

- (a) the longitudinal displacement of the helicopter from the center of the landing pad, x
- (b) the groundspeed, \dot{x}
- (c) the altitude deviation of the helicopter from the datum, h
- (d) the altitude rate, \dot{h}
- (e) the cyclic control motion, u_1 (before neuromuscular system, etc.)
- (f) the collective control motion, u_2 (before neuromuscular system, etc.)

The same index of performance was used in both the baseline and director analyses. Although it was assumed that the pilot did not use x and \dot{x} for control purposes in the director configuration, they were observable by the pilot, i.e., he could monitor these variables while using δ_{B_D} , $\dot{\delta}_{B_D}$, h and \dot{h} for control.

(3) The weighting coefficients in the index of performance were chosen as the squares of the reciprocals of the estimated maximum "allowable" deviations of the problem variables observable by the pilot.

Table 10 presents the final pilot model parameters used in the study. The nominal (a-priori) parameters differ only in the Q and R matrices. Figure 13 illustrates the comparison of RMS tracking scores for experiment and analysis. As the figure indicates, a fair comparison exists for the tracking

scores. The most serious model deficiency lies in the low predictions of the RMS values of the horizontal velocity \dot{h} . For the purposes of this study, however, the predictions were felt to be acceptable.

Discussion

The values of τ , T_N , and ρ shown in table 10 were chosen as follows: The time delay τ and neuromuscular time constant T_N were chosen as 0.2 sec rather than the 0.1 sec value used in section 2. It was felt that the larger values were more realistic and agreed more closely with values typically used in the literature. The ρ value is that recommended in the literature [1]. The noise-signal ratio ρ' was set to 0.01 for the same reason outlined previously, the nature of the control devices. The selection of the covariance for the collective residual motor noise has been discussed. The indifference thresholds represent subjective estimates. The weighting coefficients were selected on the basis of reasonable maximum allowable deviations of the pertinent variables and the ability of these deviations to yield acceptable RMS tracking scores. Only these values were changed from a-priori selections to achieve acceptable RMS performance comparisons. Based upon these comparisons, it was assumed that a dynamically representative model of the human pilot had been obtained. The pilot and model generated (via fig. 11) numerical opinion ratings are shown below.

RATINGS

Display	Pilot	Model
baseline	A6	A6.2 (J = 0.73)
director	A4	A4.2 (J = 0.40)

The correlation is quite acceptable, offering encouraging evidence that the rating hypothesis is reasonable. If one uses the experimentally determined mean RMS scores to form an index of performance equivalent to the analytical one, the resulting ratings are A6.2 and A5.2 for the baseline and director displays respectively. Again, the results are encouraging.

EXAMPLE 2. UH-1H LANDING APPROACH

Vehicle/Task Description

This task involved the simulated longitudinal control of a UH-1H unaugmented helicopter in a landing approach at a nominal 30.9 m/sec (60 kt) groundspeed on a -6° glideslope in the presence of longitudinal and vertical turbulence. Unlike the UH-1H of example 1, this vehicle had no stabilizer bar, a device attached to the rotor hub which provides pitch and roll damping. The pilot's task involves maintaining the nominal groundspeed and glideslope by using cyclic and collective control motion. Only longitudinal motion was considered.

The fixed base pilot-in-the-loop simulation of the task was conducted on the Naval Postgraduate School's hybrid computer. As in the hover task, the vehicle dynamics were simulated on the analog computer, the display was generated on a stroke-written CRT graphics terminal with the digital computer driving the display elements. Table 11 lists the vehicle aerodynamic data. Table 12 shows the turbulence spectra. Figure 14 shows the display format. The eye-to-display distance and control stick characteristics were identical to those outlined in example 1.

A second, well trained UH-1 pilot was utilized in the experiment. After considerable training, ten data runs, each of 90 sec duration, were taken. Five of the "best" runs were then selected on the basis of a weighted sum of the RMS performance measures recorded: groundspeed deviation from the nominal, u , pitch attitude, θ , time rate of change of pitch attitude, $\dot{\theta}$, deviation from glideslope, h , cyclic control motion, δ_B , and collective control motion, δ_C . No pilot opinion was elicited in this experiment. Rather, the appropriate handling quality level was deduced from [15] using the following vehicle phugoid and short-period characteristics:

$$\begin{aligned} \omega_p &= 0.41 \text{ rad/sec} & \zeta_p &= -0.15 \\ \omega_{sp} &= 1.05 \text{ rad/sec} & \zeta_{sp} &= 0.85 \end{aligned}$$

The ability of the proposed rating scheme to generate a pilot opinion consonant with the handling quality level was then ascertained.

The following level definitions are from Section 1.5 of [15], where the landing approach task under study falls into Flight Phase C:

Level 1: Flying qualities clearly adequate for the mission Flight Phase.

Level 2: Flying qualities adequate to accomplish the mission Flight Phase, but some increase in pilot workload or degradation in mission effectiveness, or both, exists.

Level 3: Flying qualities such that the aircraft can be controlled safely, but pilot workload is excessive or mission effectiveness is inadequate, or both. Category A Flight Phases can be terminated safely, and Category B and C Flight Phases can be completed.

The association between the handling qualities Levels and the Cooper-Harper scale utilized in this study is outlined in [20] as:

<u>Level</u>	<u>Cooper-Harper Scale</u>
1	1.0 - 3.5
2	3.5 - 6.5
3	6.5 - 9.0 ⁺

The specific level in which the vehicle of this study can be categorized is found from Section 3.2.2 of [15]:

Level 1: All aperiodic responses (real roots of the longitudinal characteristic equation and the lateral-directional characteristic equation) shall be stable. Oscillatory modes of frequency greater than 0.5 rad/sec shall be stable. Oscillatory modes with frequency less than or equal to 0.5 rad/sec may be unstable provided the damping ratio is less unstable than -0.10. Oscillatory modes of frequency greater than 1.1 rad/sec shall have a damping ratio of at least 0.3.

Level 2: For those Flight Phases of the operational missions of 3.1.1 for which IFR operation is required, the Level 2 requirement is the same as for Level 1. In all other cases, for Level 2, divergent modes of aperiodic response shall not double amplitude in less than 12 sec. Oscillatory modes may be unstable provided their frequency is less than or equal to 0.84 rad/sec and their time to double amplitude is greater than 12 sec. Oscillatory modes of frequency greater than 0.84 rad/sec shall be stable.

Level 3: Divergent modes of aperiodic response shall not double amplitude in less than 5 sec. Oscillatory modes may be unstable provided their frequency is less than or equal to 1.25 rad/sec and their time to double amplitude is greater than 5 sec. Oscillatory modes of frequency greater than 1.25 rad/sec shall be stable.

Adhering strictly to these criteria, one sees that the vehicle fits into Level 3:

(1) Level 1 is eliminated since the unstable oscillatory mode has a damping ratio $\zeta_p = -0.15$ which is more unstable than -0.10.

(2) Level 2 is eliminated since IFR conditions are specified, i.e., an integrated CRT display is being utilized in the simulation.

(3) Level 3 conditions are easily met since oscillatory unstable modes may have frequencies up to 1.25 rad/sec and time to double amplitude as small as 5 sec. For this vehicle's unstable mode:

$$\omega_p = 0.41 \text{ rad/sec}$$

$$T_d = \text{time to double amplitude} = 11.2 \text{ sec}$$

Optimal Pilot Modeling

With three exceptions, the general form of the pilot model for the landing approach is identical to the form of the model used to obtain the rating functions. These exceptions are:

(1) Task interference was considered in selecting the noise-signal ratios, ρ_i , for the observed variables.

(2) No indifference thresholds were utilized in the model. Instead the "full attention" noise-signal ratio, ρ , was set to 0.08 rather than 0.01.

(3) The time rate of change of groundspeed, u , was assumed not to be observed by the pilot.

The displayed quantities for the approach task are:

- (1) the groundspeed deviation from nominal, u .
- (2) pitch attitude, θ .
- (3) deviation from glideslope; h .

The perceived quantities are $\dot{\theta}$ and \dot{h} , the time derivatives of θ and h . The model for task interference, as outlined in example 1, was utilized here. Since the groundspeed symbology of figure 14 was effectively integrated into the aircraft symbol, it was assumed that there were but two displayed quantities for the purposes of task interference: θ and h . In contrast to the methods of example 1, the f_i , $i = 1, 2$, were selected on the basis of the values which minimize the index of performance subject to the constraint

$$\sum_{i=1}^2 f_i = 1.0 \quad f_i > 0 \quad i=1,2$$

It was found that $f_1 = f_2 = 0.5$.

The experimental and analytical work devoted to this landing approach task predates the work of the previous sections. The omission of display thresholds in favor of a larger full attention noise-signal ratio merely characterizes this early analysis.

As figure 14 indicates, groundspeed deviations are indicated by the pivoting "wings" on the aircraft symbol. When the proper groundspeed is achieved, the wings and aircraft symbols are colinear. It was felt that such an implicit zero reference would severely hamper rate perception. There are several analytical means of modeling this perception problem, from the inclusion of a large indifference threshold on perceived groundspeed rate to the exclusion of groundspeed rate from the list of perceived variables. For simplicity, the latter technique was used here.

Modeling Results

Again attention was paid to ensuring that the assumptions of the rating hypothesis were met.

(1) In an attempt to obtain a dynamically representative model of the human pilot, model parameters were selected so that a fair match existed between experimental and analytical RMS performance.

(2) The problem variables selected for inclusion in the index of performance were

- (a) groundspeed deviation from nominal, u .
- (b) pitch rate, $\dot{\theta}$.
- (c) the cyclic control motion, u_1 (before neuromuscular system, etc.)
- (d) the collective control motion, u_2 (before neuromuscular system, etc.)

(3) The weighting coefficients in the index of performance were chosen as the squares of the reciprocals of the estimated maximum "allowable" deviations of problem variables observable by the pilot.

Table 13 presents the pilot model parameters used in the study. Only the noise-signal ratio, ρ , and R weighting matrix choices were modified from a-priori choices to obtain acceptable RMS comparisons. Figure 15 illustrates the comparison of RMS tracking scores for experiment and analysis. As the figure indicates, a good comparison exists with the exception of $\dot{\theta}$. Despite the $\dot{\theta}$ discrepancy, the predictions were felt to be acceptable.

Discussion

The values of τ and T_N were chosen for reasons identical to those of example 1. Based upon the experimental RMS scores, the observation noise for full attention, ρ , was chosen as 0.08 (as opposed to the 0.01 value normally used). This larger value effectively compensates for the lack of indifference thresholds in the model. The motor noise, ρ' , is identical to the value recommended in [1]. Again, this analysis and experiment predate those described in the previous sections, in which indifference thresholds and a larger ρ' were utilized. The weighting coefficients for the index of performance were selected on the basis of reasonable maximum allowable deviations of the pertinent variables and the ability of these coefficients to yield acceptable RMS tracking scores. With the exception of $\dot{\theta}$, the RMS comparisons indicate a fair match. The cause of the $\dot{\theta}$ discrepancy was not determined. Based upon the RMS performance comparisons alone, it was assumed that a dynamically representative model of the human pilot had been obtained.

The actual and model generated flying qualities levels are shown below.

Flying Qualities Level

Actual	Model
Level 3 (6.5 - 9.0 ⁺)	Level 3 (6.6) (J = 0.60)

The 6.6 Cooper-Harper rating lies just within the Level 3 as described previously. Since the vehicle easily meets the Level 3 criteria, the 6.6 rating represents a very acceptable prediction. If one uses the experimentally determined mean RMS scores in an index of performance equivalent in form to

the analytical one, the resulting rating is 7.0. Again, an acceptable rating is obtained.

EXAMPLE 3. H-19 HOVER

Vehicle/Task Description

This task involved the simulated longitudinal control of an H-19 helicopter in both unaugmented and augmented configuration in hover, in the presence of longitudinal turbulence. The pilot's task involved keeping the vehicle over the center of a landing pad. The following task definition was given to the pilots:

"Hover over a spot on the ground maintaining position within ± 1.22 m (± 4 ft) using piloting techniques appropriate for VFR flight in a gusty environment. No altitude or lateral control required."

Details of the simulation can be found in [14]. Table 14 lists the vehicle aerodynamic data. Table 15 shows the turbulence spectrum. Figure 16 shows the display symbology pertinent to this study. No eye-to-display distance was stated in [14]. The control stick was a standard aircraft-type center stick with a force gradient of 2.4 newtons/cm. The data for a single pilot (denoted pilot 's' in [14]) was used. Two H-19 configurations were utilized. One, an unaugmented vehicle, the second, a vehicle with an attitude augmentation system as outlined in table 14.

Optimal Pilot Modeling

With two exceptions, the general form of the optimal pilot model was identical to the form of the model used to obtain the rating functions. These exceptions are:

(1) The pilot's effective time delay was modeled by a first-order Pade' approximation:

$$e^{-\tau s} = - \frac{(s - 2/\tau)}{(s + 2/\tau)}$$

(2) Task interference was considered in selecting the noise-signal ratios, ρ_i , for the observed variables.

The displayed quantities for the hover task are:

(1) the longitudinal displacement of the helicopter from the center of the landing pad, x .

(2) the pitch attitude, θ .

The perceived quantities are \dot{x} and $\dot{\theta}$, the time derivatives of the displayed quantities. Equal allocation of attention between the displayed quantities x and θ was assumed. Thus

$$f_t = 1.0 \quad f_s = 1.0 \quad f_i = 0.5 \quad i = 1,2$$

Modeling Results

Again, attention was paid to ensuring that the assumptions of the rating hypothesis were met:

(1) In an attempt to obtain dynamically representative models of the human pilot, model parameters were selected so that a fair match existed between experimental and analytical RMS error scores.

(2) The problem variables selected for inclusion in the index of performance were:

- (a) longitudinal displacement of the helicopter from the center of the landing pad, x .
- (b) the groundspeed, \dot{x} .
- (c) the cyclic control motion, u (before neuromuscular system, etc.)

(3) The weighting coefficients in the index of performance were chosen as the squares of the reciprocals of the estimated maximum "allowable" deviations of problem variables observable by the pilot.

Table 16 presents the final pilot model parameters used in the study. Considerable adjustments in the a-priori values of the Q and R matrices and indifference thresholds were needed to achieve acceptable RMS performance comparisons. Figure 17 illustrates the comparison of RMS tracking scores for experiment and analysis. The experimental scores and corresponding ratings are from the first two runs of pilot 's' in [14]. As the figure indicates, a good comparison exists. As table 16 shows, only the pilot indifference thresholds were changed in going from the unaugmented to the augmented vehicle.

Discussion

The values of τ , T_N , ρ , and ρ' in table 16 were chosen identical to those of example 1. The weighting coefficients for the index of performance and the thresholds were selected so as to yield acceptable RMS performance comparisons with experiment. The final maximum allowable deviations and indifference thresholds for this example are, in general, much smaller than those for the UH-1H hover task of example 1. These smaller values are a reflection of the fact that the RMS performance scores are much lower for the H-19 than for the UH-1H vehicle. On the basis of the performance comparisons of figure 17, it was assumed that a dynamically representative model of the pilot

had been obtained. The pilot and model generated numerical opinion ratings are shown below.

RATINGS

Vehicle	Pilot	Model
H-19	U8	U8 (J = 2.63)
H-19AA (augmented)	A4.5 - 5.0	A5 (J = 0.48)

If the experimentally determined mean RMS scores are used in an index of performance equivalent in form to the analytical one, ratings of 9.0 and 5.5 are obtained. While these values are somewhat high, they are still acceptable.

CONCLUSIONS AND RECOMMENDATIONS

It was the purpose of this study to test the rating hypothesis by modeling the human pilot in four specific flight tasks in which experimental RMS performance measures and pilot ratings were available or could be inferred. In general, the results indicate that the hypothesis is reasonable. More correlation between experimental and analytical work along the lines of examples 1-3 is obviously needed. However, even if positive correlations are forthcoming, the ability to use the rating scheme in a predictive capacity still will hinge upon discerning whether the criteria stated in the rating hypothesis have been met. Even with simulation results (RMS performance, describing functions, etc.), this can involve a good deal of educated guessing. For example, the modeling of the pilot in the UH-1H baseline experiment required seventeen parameters to be specified (see table 10). The situation is further aggravated by the fact that no procedure now exists for identifying all the optimal pilot model parameters from simulation data [21]. The majority of modeling to date has been accomplished in a manner similar to that pursued here, i.e., RMS performance matching.

Thus the potential of the analytical rating technique which has been discussed is eroded by the lack of a well defined procedure for selecting pilot model parameters, a priori, given a specific vehicle and task, and by the inability to identify these pilot model parameters, a posteriori, given simulation data. One can, however, suggest a procedure for selecting the parameters which minimizes the guesswork involved:

- (1) Select τ , T_N , ρ , and ρ' as

$$\tau = T_N = 0.2 \text{ sec}$$

$$\rho = \rho' = 0.01$$

- (2) Select the maximum allowable deviations of each observed variable in the index of performance as that deviation producing a display indicator

movement which subtends a specific visual arc or arc rate, at the pilot's eye. The data of this study indicate that 1-2 deg and 1-2 deg/sec appear to be reasonable values. For the control movement, select the maximum allowable deviation as a specific percentage of the maximum control motion possible, 25 percent being a reasonable figure.

(3) Select the indifference thresholds on each observed variable to be a specific percentage of the visual arc and arc rate selected in (2). Here again, 25 percent would be a reasonable value. Do not allow these threshold values to be smaller than the thresholds associated with visual discrimination, i.e., 0.05 deg and 0.05 deg/sec.

(4) Use the model for task interference to select the fraction of attention for each observed variable. This means finding that set f_i which minimizes the index of performance subject to the constraints

$$\sum_{i=1}^n f_i = 1.0 \quad f_i > 0 \quad i = 1, 2, \dots, n$$

(5) Use the rating scheme to predict general flying qualities levels, as done in example 2, rather than specific numerical ratings.

A positive demonstration of the utility of this parameter selection procedure would significantly enhance the rating scheme offered in this report.

REFERENCES

- [1] Kleinman, D. L.; Baron, S.; and Levison, W. H.: An Optimal Control Model of Human Response, Parts I and II, Automatica, vol. 6, May 1970, pp. 357-383.
- [2] Kleinman, D. L.; and Baron, S.: Analytic Evaluation of Display Requirements for Approach to Landing, NASA CR-1952, November 1971.
- [3] Kleinman, D. L.; and Killingsworth, W. R.: A Predictive Pilot Model for STOL Aircraft Landing, NASA CR-2374, March 1974.
- [4] Baron, S.; and Levison, W. H.: A Display Evaluation Methodology Applied to Vertical Situation Displays, Proceedings of the Ninth Annual Conference on Manual Control, May 1973, pp. 121-132.
- [5] Wewerinke, P. H.: Human Operator Workload for Various Control Situations, Proceedings of the Tenth Annual Conference on Manual Control, April 1974, pp. 167-192.
- [6] Cooper, G. E.: Understanding and Interpreting Pilot Opinion, Aeronautical Engineering Review, vol. 16, no. 3, March 1957, pp. 47-52.

- [7] Cooper, G. E.; and Harper, R. P., Jr.: The Use of Pilot Rating in the Evaluation of Aircraft Handling Qualities, NASA TN D-5153, April 1969.
- [8] Anderson, R. O.: A New Approach to the Specification and Evaluation of Flying Qualities, AFFDL-TR-69-120, June 1970.
- [9] Adams, J. J.; and Hatch, H. G., Jr.: An Approach to the Determination of Aircraft Handling Qualities by Using Pilot Transfer Functions, NASA TN D-6104, January 1971.
- [10] Onstott, E. D., et al.: Prediction and Evaluation of Flying Qualities in Turbulence, AFFDL-TR-70-143, February 1971.
- [11] McRuer, D. T.; and Jex, H. R.: A Review of Quasi-Linear Pilot Models, IEEE Transactions on Human Factors in Electronics, vol. HFE 8, no. 3, September 1967, pp. 231-249.
- [12] Bryson, A. E.; and Ho, Y. C.: Applied Optimal Control, Blaisdell Publishing Co., 1969, p. 149.
- [13] McDonnell, J. D.: Pilot Rating Techniques for the Estimation and Evaluation of Handling Qualities, AFFDL-TR-68-76, December 1968.
- [14] Teper, G. L.: An Assessment of the "Paper Pilot" - An Analytical Approach to the Specification and Evaluation of Flying Qualities, AFFDL-TR-71-174, June 1972.
- [15] Anon.: Military Specification - Flying Qualities of Piloted V/STOL Aircraft, MIL-F-83300, December 1970.
- [16] McRuer, D. T.; and Graham, D.: Analysis of Nonlinear Control Systems, John Wiley and Sons, 1961, pp. 230-244.
- [17] Levison, W. H.; Elkind, J. I.; and Ward, J. L.: Studies of Multivariable Manual Control Systems: A Model for Task Interference, NASA CR-1746, May 1971.
- [18] Levison, W. H.: A Model-Based Technique for the Design of Flight Directors, Proceedings of the Ninth Annual Conference on Manual Control, May 1973, pp. 163-172.
- [19] Curry, R. E.; Kleinman, D. L.; and Hoffman, W. C.: A Model for Simultaneous Monitoring and Control, Proceedings of the Eleventh Annual Conference on Manual Control, May 1975, pp. 144-150.
- [20] Chalk, C. R., et al.: Background Information and User Guide for MIL-F-83300 - Military Specification - Flying Qualities of Piloted V/STOL Aircraft, AFFDL-TR-70-88, March 1971, p. 39.
- [21] Phatak, A.; Weinert, H.; and Segall, I.: Identification of the Optimal Control Model for the Human Operator, AMRL TR-74-79, September 1974.

TABLE 1.- INPUT SINUSOIDS FROM [13]

Component no.	Component frequency (rad/sec)	Component amplitude A_i (cm)
1	0.188	0.566
2	.314	
3	.502	
4	.816	
5	1.19	
6	1.88	
7	2.89	
8	4.77	
9	7.35	
10	9.23	
11	12.2	
12	15.0	

TABLE 2.- CONTROLLED ELEMENTS FOR EXPERIMENTS AND MODELING OF [13]

Controlled element		K_B (cm/cm-sec ⁿ)*	a	b (rad/sec)
Ref. [13]	Modeling			
K_B/s	$K_B a/s(s + b)$	0.586	40.	40.
$K_B/s(s + 4)$		2.15	1.	4.
$K_B/s(s + 2)$		2.15	1.	2.
$K_B/s(s + 1)$		2.15	1.	1.
K_B/s^2		1.17	1.	0.
$0.1K_B/s^2$		1.17	.1	0.
$10.0K_B/s^2$		1.17	10.0	0.

*Here n refers to the exponent on the free s in the denominator of the transfer function of the controlled element.

TABLE 3.- THE ORIGINAL COOPER SCALE

COOPER					PR
Description	Adjective rating	Mission	Primary mission accomplished?	Can be landed?	
Excellent, includes optimum	Satisfactory	Normal operation	Yes	Yes	1.
Good, pleasant to fly			Yes	Yes	2
Satisfactory, but with some mildly unpleasant characteristics			Yes	Yes	3
Acceptable, but with unpleasant characteristics	Unsatisfactory	Emergency operation	Yes	Yes	4
Unacceptable for normal operation			Doubtful	Yes	5
Acceptable for emergency operation (stab. aug. failure) only			Doubtful	Yes	6
Unacceptable even for emergency condition (stab. aug. failure)	Unacceptable	No operation	No	Doubtful	7
Unacceptable-dangerous			No	No	8
Unacceptable-uncontrollable			No	No	9
0 !! Did not get back to report	Unprintable	What mission?			10

TABLE 4.- THE REVISED COOPER-HARPER SCALE

26	Controllable Capable of being controlled or managed in context of mission, with available pilot attention	Acceptable May have deficiencies which warrant improvement, but adequate for mission.	Satisfactory Meets all requirements and expectations, good enough with improvement.	Excellent, highly desirable.	A1
			Clearly adequate for mission.	Good, pleasant, well behaved.	A2
				Fair. Some mildly unpleasant characteristics. Good enough for mission without improvement.	A3
		Pilot compensation, if required to achieve acceptable performance, is feasible.	Unsatisfactory Reluctantly acceptable. Deficiencies which warrant improvement. Performance adequate for mission with feasible pilot compensation.	Some minor but annoying deficiencies. Improvement is requested. Effect on performance is easily compensated for by pilot.	A4
			Very objectionable deficiencies. Major improvements are needed. Requires best available pilot compensation to achieve acceptable performance.	Moderately objectionable deficiencies. Improvement is needed. Reasonable performance requires considerable pilot compensation.	A5
				Major deficiencies which require mandatory improvement for acceptance. Controllable. Performance inadequate for mission, or pilot compensation required for minimum acceptable performance in mission is too high.	A6
	Unacceptable Deficiencies which require mandatory improvement. Inadequate performance for mission even with maximum feasible pilot compensation.		Controllable with difficulty. Requires substantial pilot skill and attention to retain control and continue mission.	U7	
			Marginally controllable in mission. Requires maximum available pilot skill and attention to retain control.	U8	
				U9	
Uncontrollable Control will be lost during some portion of mission.			Uncontrollable in mission	10	

TABLE 5.- MATRIX DEFINITIONS FOR MODELING OF EXPERIMENTS FROM [13]

x(t) vector

$$\left. \begin{array}{l} x_1(t) = \theta(t) = \text{controlled element output} \\ x_2(t) = \dot{x}_1(t) = \dot{\theta}(t) \\ \left. \begin{array}{l} x_3(t) \\ x_4(t) \end{array} \right\} \text{Pade' approximation states} \\ x_5(t) = \delta_e(t) = \text{control stick motion} \\ x_6(t) = \theta_c(t) = \text{command input} \\ x_7(t) = \dot{x}_6(t) = \dot{\theta}_c(t) \end{array} \right\}$$

A matrix

$$\begin{bmatrix} 0 & 1 & 0 & 0 & 0 & 0 & 0 \\ 0 & -b & 0 & 0 & K_B a & 0 & 0 \\ 0 & 0 & 0 & 1.0 & 0 & 0 & 0 \\ 0 & 0 & -16/\tau^2 & -8/\tau & 0 & 0 & 0 \\ 0 & 0 & 1/T_N & 0 & -1/T_N & 0 & 0 \\ 0 & 0 & 0 & 0 & 0 & 0 & 1 \\ 0 & 0 & 0 & 0 & 0 & -2.25 & -3. \end{bmatrix}$$

B matrix

$$\begin{Bmatrix} 0 \\ 0 \\ -16/\tau \\ 128/\tau^2 \\ 1/T_N \\ 0 \\ 0 \end{Bmatrix}$$

u(t) vector

$$\left\{ \begin{array}{l} u_1(t) = u(t) = \text{pilot's control motion before time} \\ \text{delay and neuromuscular dynamics} \\ \text{are encountered} \end{array} \right\}$$

TABLE 5.- MATRIX DEFINITIONS FOR MODELING OF EXPERIMENTS FROM [13] - Concluded

Y matrix

$$\begin{bmatrix} 0 & 0 \\ 0 & 0 \\ 0 & 0 \\ 0 & 0 \\ 0 & 1/T_N \\ 0 & 0 \\ 3.674 & 0 \end{bmatrix}$$

w(t) vector

$$\left\{ \begin{array}{l} w_1(t) = w(t) = \text{shaping filter input} \\ w_2(t) = v_m(t) = \text{motor noise} \end{array} \right\}$$

F matrix

$$\begin{bmatrix} 1.0 & 0 \\ 0 & \rho' \pi E[u_1^2(t)] \end{bmatrix}$$

z'(t) vector

$$\left\{ \begin{array}{l} z_1'(t) = \theta_c(t) - \theta(t) = \text{displayed } \theta_e(t) \\ z_2'(t) = \dot{\theta}_c(t) - \dot{\theta}(t) = \text{perceived } \dot{\theta}_e(t) \end{array} \right\}$$

v(t) vector

$$\left\{ \begin{array}{l} v_1(t) = \text{additive noise associated with } \theta_e(t) \\ v_2(t) = \text{additive noise associated with } \dot{\theta}_e(t) \end{array} \right\}$$

H matrix

$$\begin{bmatrix} -1 & 0 & 0 & 0 & 0 & 1 & 0 \\ 0 & -1 & 0 & 0 & 0 & 0 & 1 \end{bmatrix}$$

G matrix

$$\begin{bmatrix} \rho \pi E[z_1'^2(t)] & 0 \\ 0 & \rho \pi E[z_2'^2(t)] \end{bmatrix}$$

TABLE 6.- NOMINAL PILOT MODEL PARAMETERS FOR MODELING
OF EXPERIMENTS FROM [13]

Time delay	τ	0.1 sec
Neuromuscular time constant	T_N	.1 sec
Observation noise noise-signal ratio	ρ	.01
Motor noise noise-signal ratio	ρ'	.01
Error indifference threshold	$\theta_{e_{TH}}$.5 cm of display element movement
Error rate indifference threshold	$\dot{\theta}_{e_{TH}}$.5 cm/sec of display element movement
<u>Q</u> matrix coefficient	$q_{11} = 1/(\theta_{e_m})^2$	$1/(1 \text{ cm})^2$
<u>R</u> matrix coefficient	$r_{11} = 1/(u_m)^2$	$1/(10 \text{ cm})^2$ *

*In conforming to the convention of [13], problem variables are expressed in terms of equivalent indicator movement.

TABLE 7.- FINAL PILOT MODEL PARAMETERS FOR MODELING OF EXPERIMENTS FROM [13]

Controlled Element	Model parameters which differ from nominal (Table 6)	
K_B/s		$\rho' = 0.02$
$K_B/s(s + 4)$		Same as nominal
$K_B/s(s + 2)$		Same as nominal
$K_B/s(s + 1)$		$\rho' = 0.0075$
K_B/s^2		$\rho' = .0075$
$0.1 K_B/s^2$	$\theta_{e_{TH}} = 2 \text{ cm},$	$\dot{\theta}_{e_{TH}} = 2 \text{ cm/sec}, \rho' = 0.0075$
$10.. K_B/s^2$		$\rho' = 0.0025$

TABLE 8.- NORMALIZED UH-1H LONGITUDINAL DERIVATIVES IN STABILITY AXIS SYSTEM, HOVER

$m = 3,856 \text{ kg}$	$M_u = 0.00314 \text{ /sec-m}$
$U_0 = 0 \text{ m/sec}$	$M_w = -.00477 \text{ /sec-m}$
$I_{yy} = 17,279 \text{ kg-m}^2$	$M_{\dot{w}} = 0 \text{ /m}$
$X_u = -0.00934 \text{ /sec}^*$	$M_q = -2.03 \text{ /sec}$
$X_w = -.000418 \text{ /sec}$	$X_{\delta_B} = 12.5 \text{ /sec}^2$
$X_q = 5.88 \text{ m/sec}$	$X_{\delta_C} = .00187 \text{ /sec}^2$
$Z_u = -.00214 \text{ /sec}$	$Z_{\delta_B} = -.308 \text{ /sec}^2$
$Z_w = -.404 \text{ /sec}$	$Z_{\delta_C} = -96.1 \text{ /sec}^2$
$Z_q = .462 \text{ m/sec}$	$M_{\delta_B} = -4.20 \text{ /m-sec}^2$
	$M_{\delta_C} = 0 \text{ /m-sec}^2$

*Force and moment derivatives are normalized with respect to mass and moment of inertia, e.g.,

$$X_u = \left. \frac{1}{m} \frac{\partial X}{\partial u} \right)_0 \quad M_u = \left. \frac{1}{I_{yy}} \frac{\partial M}{\partial u} \right)_0$$

TABLE 9.- TURBULENCE SPECTRUM FOR UH-1H HOVER

$$\Phi_{u_g u_g}(\omega) = \frac{\sigma_{u_g}^2 L_u}{U_0} \frac{1}{1 + (L_u \omega / U_0)^2} \text{ m}^2\text{-rad/sec}^2$$

$$\sigma_{u_g} = 1.52 \text{ m/sec (5 ft/sec)}$$

$$L_u / U_0 = 3.33 \text{ sec}^*$$

*Although $U_0 = 0$ and the "frozen turbulence" hypothesis is, strictly speaking, no longer valid, the general form of the turbulence spectrum above is retained. For example, one can consider $U_0 = 1.52 \text{ m/sec}$, $L_u = 5.06 \text{ m}$.

TABLE 10.- FINAL PILOT MODEL PARAMETERS FOR MODELING
OF UH-1H HOVER TASK

Time delay	τ	0.2 sec	
Neuromuscular time constant	T_N	.2 sec	
Observation noise noise-signal ratio (full attention)	ρ	.01	
Motor noise noise-signal ratio	ρ'	.01	
Covariance of collective residual motor noise	$E[r^2(t)]$		
baseline			$(1.0 \text{ cm})^2$
director			$(.75 \text{ cm})^2$
Baseline indifference thresholds			
	x_{TH}	0.305 m (1 ft)	(.00133 rad visual arc)
	\dot{x}_{TH}	0.914 m/sec (3 ft/sec)	(.00399 rad/sec visual arc)
	h_{TH}	0.305 m (1 ft)	(.000667 rad visual arc)
	\dot{h}_{TH}	0.914 m/sec (3 ft/sec)	(.00199 rad/sec visual arc)
	θ_{TH}	0.0175 rad (1 deg)	(.00166 rad visual arc)
	$\dot{\theta}_{TH}$	0.0525 rad/sec (3 deg/sec)	(.005 rad/sec visual arc)
Director indifference thresholds			
	$\delta_{B_{D_{TH}}}$		(.00166 rad visual arc)
	$\dot{\delta}_{B_{D_{TH}}}$		(.005 rad/sec visual arc)
	h_{TH}	0.305 m (1 ft)	(.000667 rad visual arc)
	\dot{h}_{TH}	0.914 m/sec (3 ft/sec)	(.00199 rad visual arc)

TABLE 10.- FINAL PILOT MODEL PARAMETERS FOR MODELING
OF UH-1H HOVER TASK - Concluded

<u>Q</u> matrix coefficients		
baseline	$q_{11} = 1/(\dot{x}_M)^2$	$1/(1.52 \text{ m/sec})^2$ $(1/(5 \text{ ft/sec})^2)$
	$q_{22} = 1/(\dot{h}_M)^2$	$1/(7.62 \text{ m/sec})^2$ $(1/(25 \text{ ft/sec})^2)$
	$q_{33} = 1/(x_M)^2$	$1/(7.62 \text{ m})^2$ $(1/(25 \text{ ft/sec})^2)$
	$q_{44} = 1/(\dot{h}_M)^2$	$1/(3.05 \text{ m/sec})^2$ $(1/(10 \text{ ft/sec})^2)$

<u>O</u> matrix coefficients		
director	same as baseline	

<u>R</u> matrix coefficients		
baseline	(cyclic) $r_{11} = 1/(u_{1M})^2$	$1/(6.10 \text{ cm})^2$ $(1/(.2 \text{ ft})^2)$
	(collective) $r_{22} = 1/(u_{2M})^2$	$1/(3.05 \text{ cm})^2$ $(1/(.1 \text{ ft})^2)$
director	same as baseline	

TABLE 11.- NORMALIZED UH-1H LONGITUDINAL DERIVATIVES IN
STABILITY AXIS SYSTEM, LANDING APPROACH

$m = 3,856 \text{ kg}$	$M_u = 0.0149 \text{ /sec-m}$
$U_0 = 30.9 \text{ m/sec (60 kts)}$	$M_w = -0.00155 \text{ /sec-m}$
$I_{yy} = 17,279 \text{ kg-m}^2$	$M_{\dot{w}} = 0. /m$
$X_u = -0.0242 \text{ /sec}^*$	$M_q = -0.455 \text{ /sec}$
$X_w = 0.00603 \text{ /sec}$	$X_{\delta_B} = 12.1 \text{ /sec}^2$
$X_q = 0.472 \text{ m/sec}$	$X_{\delta_C} = 0.787 \text{ /sec}^2$
$Z_u = -0.0719 \text{ /sec}$	$Z_{\delta_B} = 47.1 \text{ /sec}^2$
$Z_w = -1.17 \text{ /sec}$	$Z_{\delta_C} = -186. \text{ /sec}^2$
$Z_q = -0.272 \text{ m/sec}$	$M_{\delta_B} = -5.18 \text{ /m-sec}^2$
	$M_{\delta_C} = 0. \text{ /m-sec}^2$

*Force and moment derivatives are normalized with respect to mass and moment of inertia, e.g.,

$$X_u = \frac{1}{m} \frac{\partial X}{\partial u} \Big|_0$$

$$M_u = \frac{1}{I_{yy}} \frac{\partial M}{\partial u} \Big|_0$$

TABLE 12.- TURBULENCE SPECTRA FOR UH-1H LANDING APPROACH

Vertical Turbulence

$$\Phi_{w_g w_g}(\omega) = \frac{2\sigma_w^2 L_w}{U_0} \frac{1}{1 + (L_w \omega / U_0)^2} \text{ m}^2\text{-rad/sec}^2$$

$$\sigma_{w_g} = 1.52 \text{ m/sec (5 ft/sec)}$$

$$L_w = 30.5 \text{ m (100 ft)}$$

$$U_0 = 30.9 \text{ m/sec (60 kts)}$$

Horizontal Turbulence

$$\Phi_{u_g u_g}(\omega) = \frac{2\sigma_u^2 L_u}{U_0} \frac{1}{1 + (L_u \omega / U_0)^2} \text{ m}^2\text{-rad/sec}^2$$

$$\sigma_{u_g} = 1.52 \text{ m/sec (5 ft/sec)}$$

$$L_u = 183. \text{ m (600 ft)}$$

TABLE 13.- FINAL PILOT MODEL PARAMETERS FOR MODELING
OF UH-1H LANDING APPROACH TASK

Time delay	τ	0.2 sec
Neuromuscular time constant	T_N	.2 sec
Observation noise noise-signal ratio (full attention)	ρ	.08
Motor noise noise-signal ratio	ρ'	.003
Q matrix coefficients	$q_{11} = 1/(u_M)^2$ $q_{22} = 1/(\dot{\theta}_M)^2$ $q_{33} = 1/(h_M)^2$	$1/(3.05 \text{ m/sec})^2$ $(1/(10 \text{ ft/sec})^2)$ $1/(0.04 \text{ rad/sec})^2$ $1/(3.05 \text{ m})$ $(1/(10 \text{ ft/sec})^2)$
<u>R</u> matrix coefficients	(cyclic) $r_{11} = 1/(u_{1M})^2$ (collective) $r_{22} = 1/(u_{2M})^2$	$1/(7.62 \text{ cm})^2$ $(1/(0.25 \text{ ft})^2)$ $1/(3.05 \text{ cm})$ $(1/(0.1 \text{ ft})^2)$

TABLE 14. NORMALIZED H-19 LONGITUDINAL DERIVATIVES IN
STABILITY AXIS SYSTEM, HOVER

$m = 2,892 \text{ kg}$	$M_u = 0.0199 \text{ sec/m}$
$U_0 = 0 \text{ m/sec}$	$M_q = -.61 \text{ /sec}$
$I_{yy} = 13,080 \text{ kg-m}^2$	$X_\delta = -26.4 \text{ /sec}^2$
$X_u = -0.0284 \text{ /sec}^*$	$M_\delta = 17.9 \text{ /m-sec}^2$
$X_q = 0 \text{ m/sec}$	$K_\delta = .27 \text{ cm/cm}^{**} \text{ (0.41 cm/cm in augmented eqns)}$

Augmentation Equation

$$\delta_A = \delta - K_\theta \theta - K_u u$$

$$K_u = 0 \text{ /sec} \quad K_\theta = 10.$$

*Force and moment derivatives are normalized with respect to mass and moment of inertia, e.g.,

$$X_u = \frac{1}{m} \left. \frac{\partial X}{\partial u} \right)_0 \quad M_u = \frac{1}{I_{yy}} \left. \frac{\partial M}{\partial u} \right)_0$$

**Control-stick gain.

TABLE 15.- TURBULENCE SPECTRUM FOR H-19 HOVER

$$\Phi_{u_g u_g}(\omega) = \frac{0.379}{\omega^2 + 0.0985} \text{ m}^2\text{-rad/sec}^2$$

turbulence intensity = 0.777 m/sec (2.55 ft/sec)

TABLE 16.- FINAL PILOT MODEL PARAMETERS FOR MODELING OF H-19 HOVER TASK

Time delay	τ	0.2 sec
Neuromuscular time constant	T_N	.2 sec
Observation noise noise-signal ratio	ρ	:01
Motor noise noise-signal ratio	ρ'	.01
Indifference thresholds		
unaugmented vehicle	x_{TH}	0.012 m (0.04 ft)
	\dot{x}_{TH}	0.036 m/sec (0.12 ft/sec)
augmented vehicle	x_{TH}	0.036 m (0.12 ft)
	\dot{x}_{TH}	0.073 m/sec (0.24 ft/sec)
	θ_{TH}	0.01 rad
	$\dot{\theta}_{TH}$	0.01 rad/sec
<u>Q</u> matrix coefficients	$q_{11} = 1/(x_M)^2$	$1/(0.305 \text{ m})^2$ $(1/(1 \text{ ft})^2)$
	$q_{22} = 1/(\dot{x}_M)^2$	$1/(0.061 \text{ m/sec})^2$ $(1/(0.2 \text{ ft/sec})^2)$
<u>R</u> matrix coefficients	$r_{11} = 1/(u_M)^2$	$1/(1.22 \text{ cm})^2$ $(1/(0.04 \text{ ft})^2)$

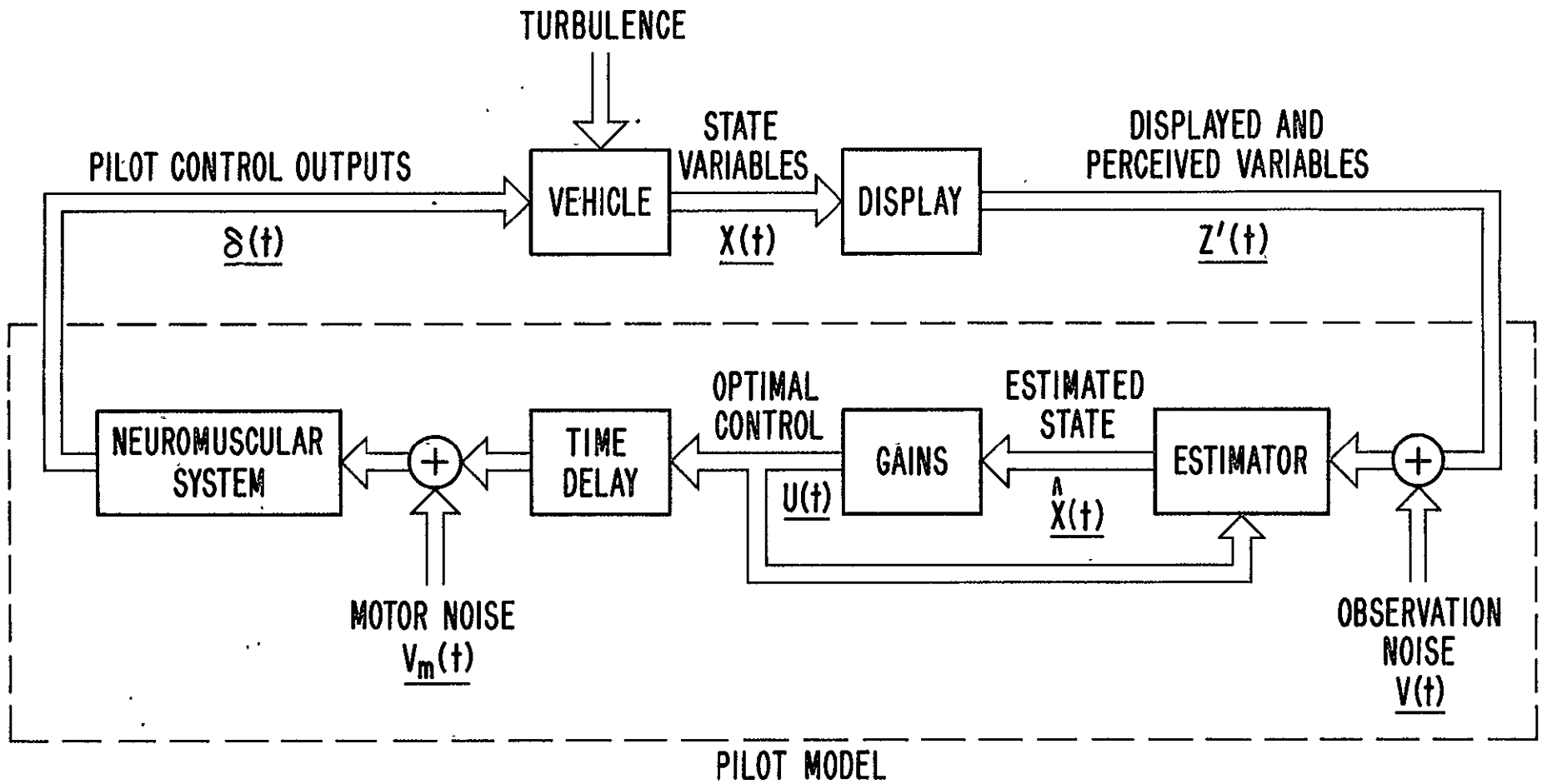


Figure 1.- Block diagram of pilot-vehicle system.

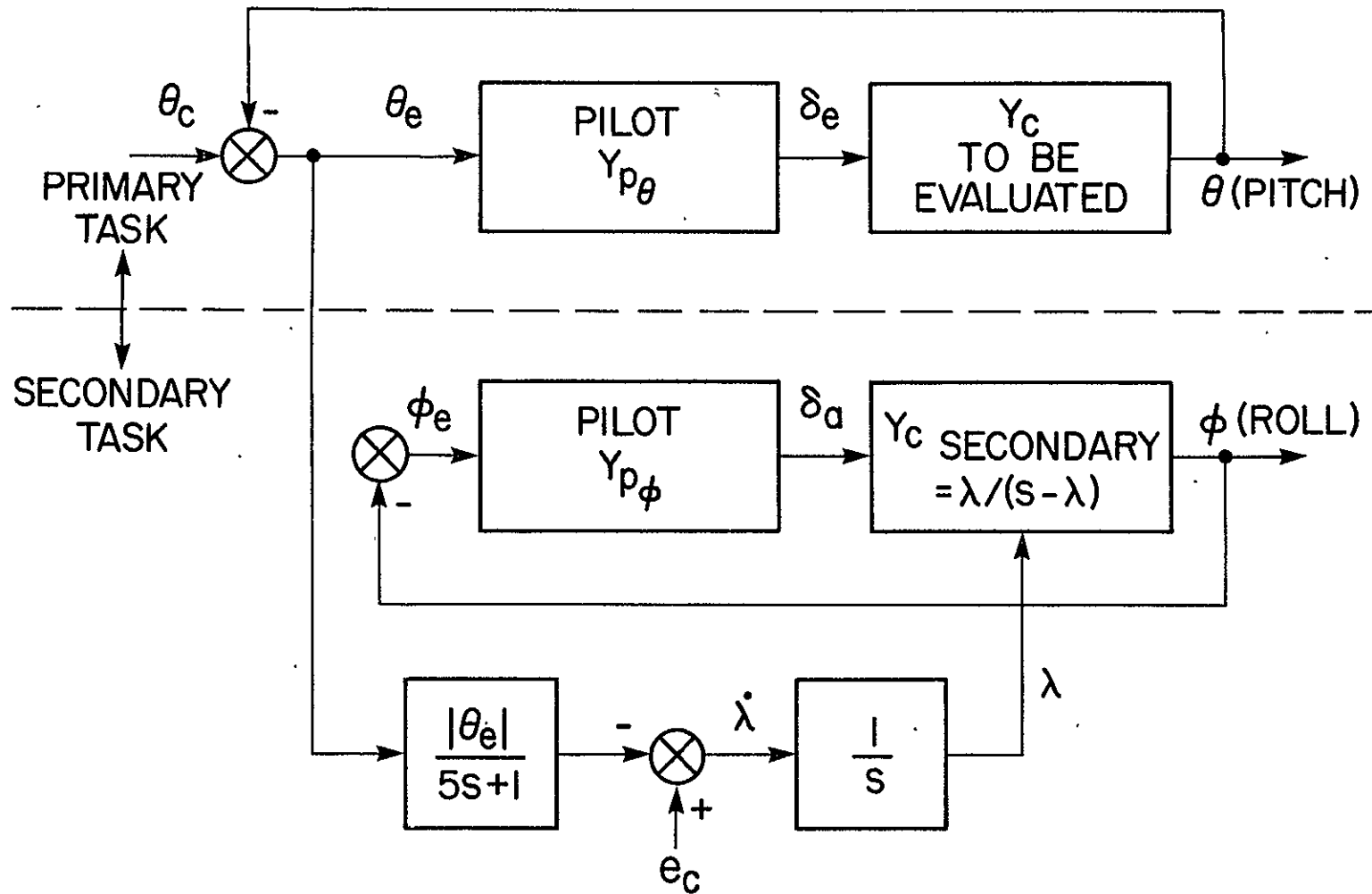
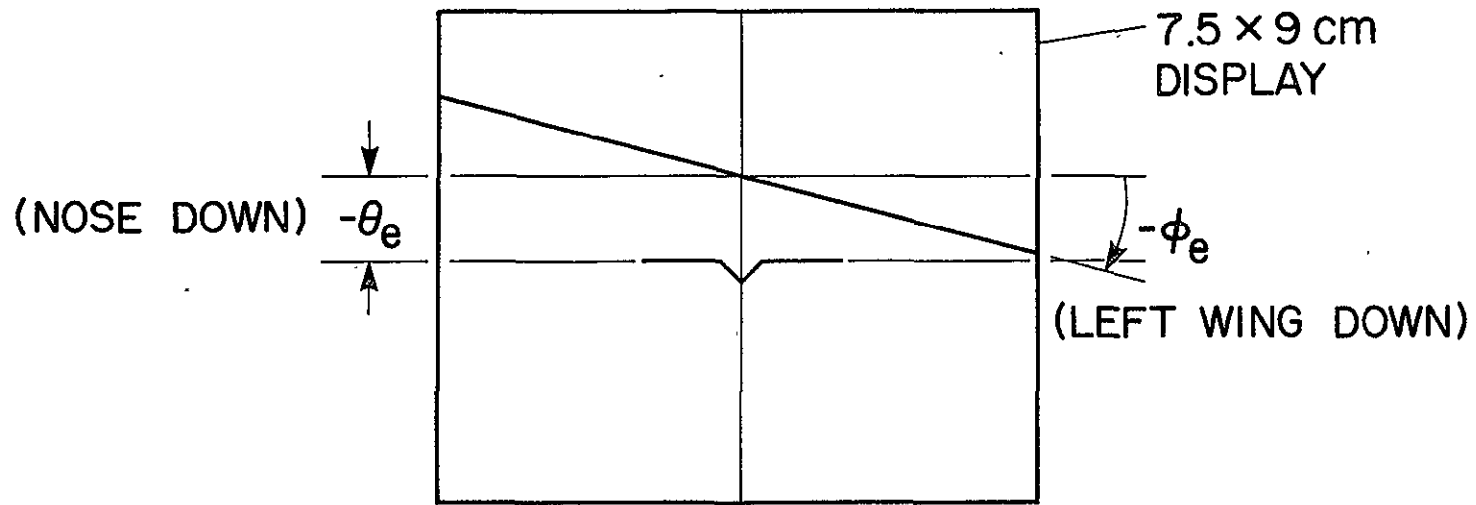


Figure 2.- Single-loop primary task with secondary cross-coupled loading task from [13].



DISPLAY LIMITS

$$\theta \doteq \pm 3.75 \text{ cm}$$

$$\phi \doteq \pm 45 \text{ deg}$$

Figure 3.- CRT display for single-loop plus secondary tasks from [13].

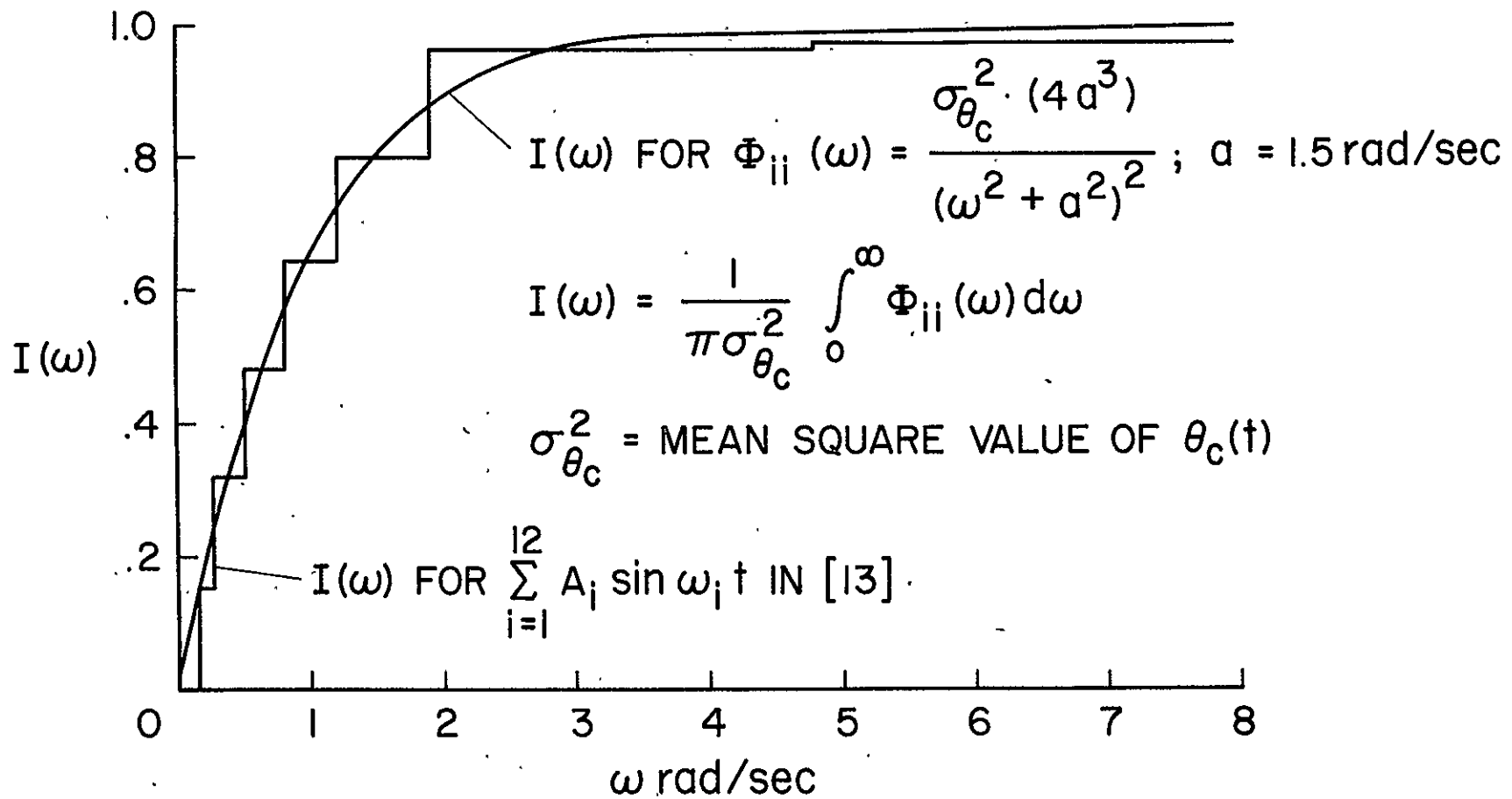


Figure 4.- Input matching for model and experiments from [13].

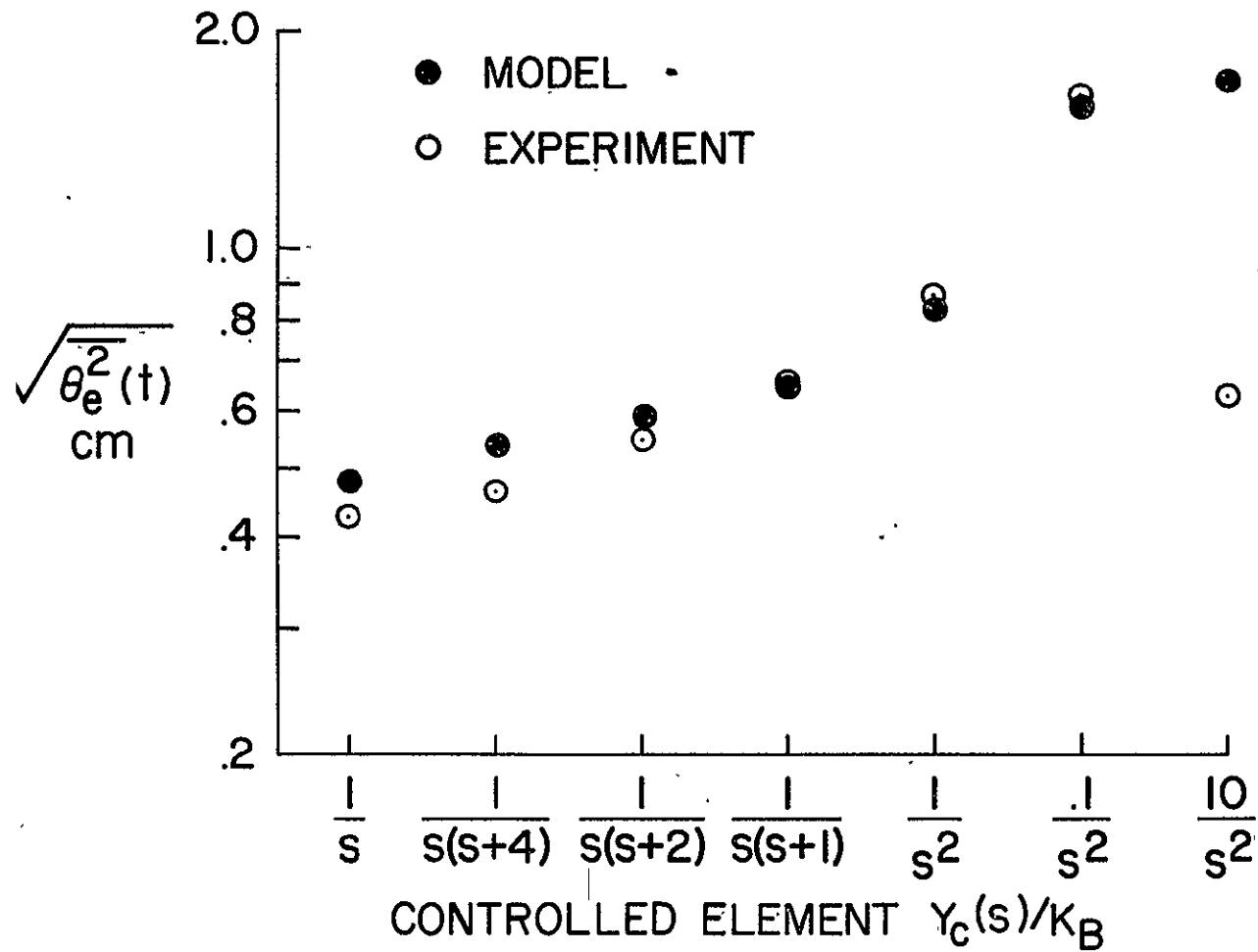


Figure 5.- Comparison of model generated and experimental tracking errors for experiments from [13].

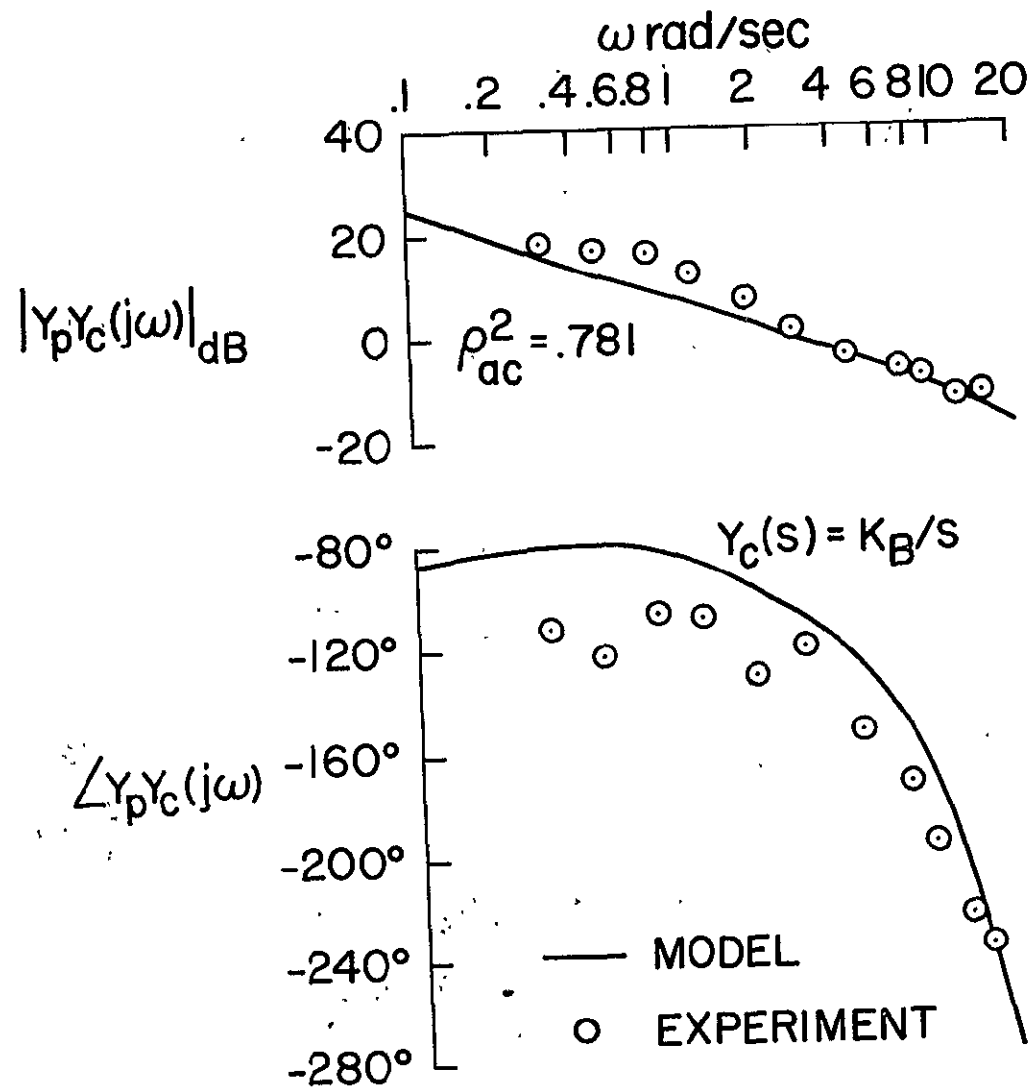


Figure 6.- A comparison of model generated and experimental open-loop describing functions for experiments from [13].

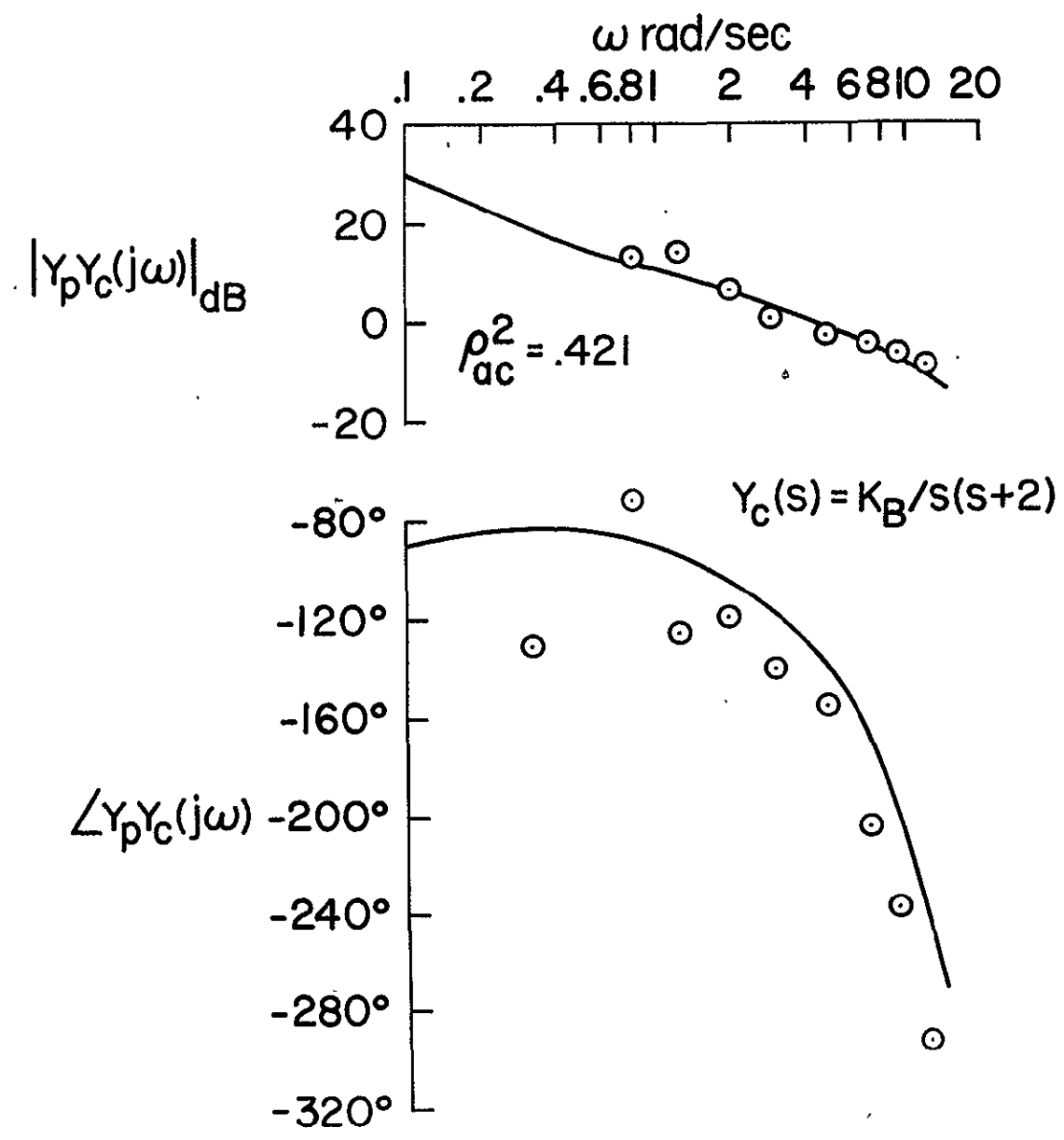


Figure 7.- A comparison of model generated and experimental open-loop describing functions for experiments from [13].

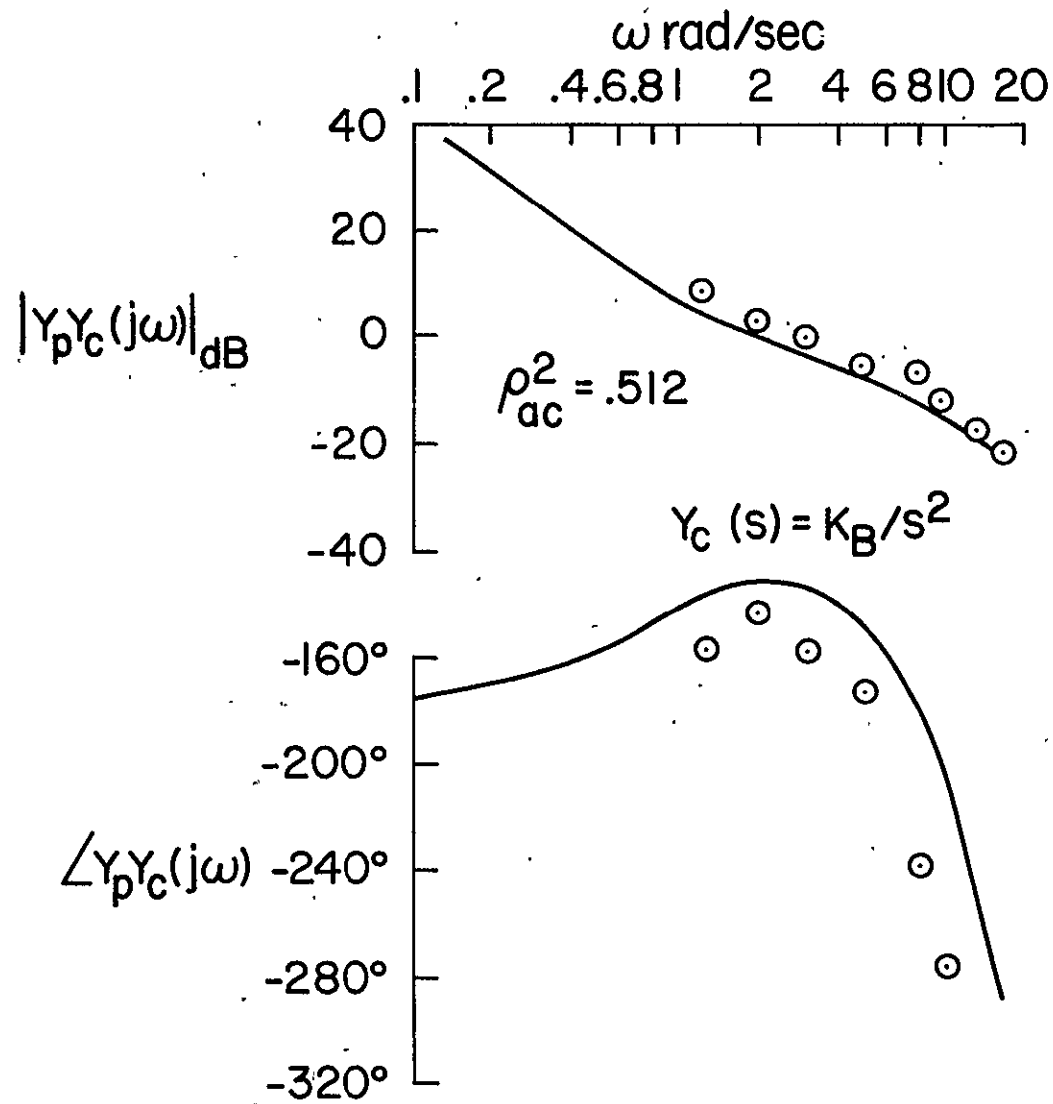


Figure 8.- A comparison of model generated and experimental open-loop describing functions for experiments from [13].

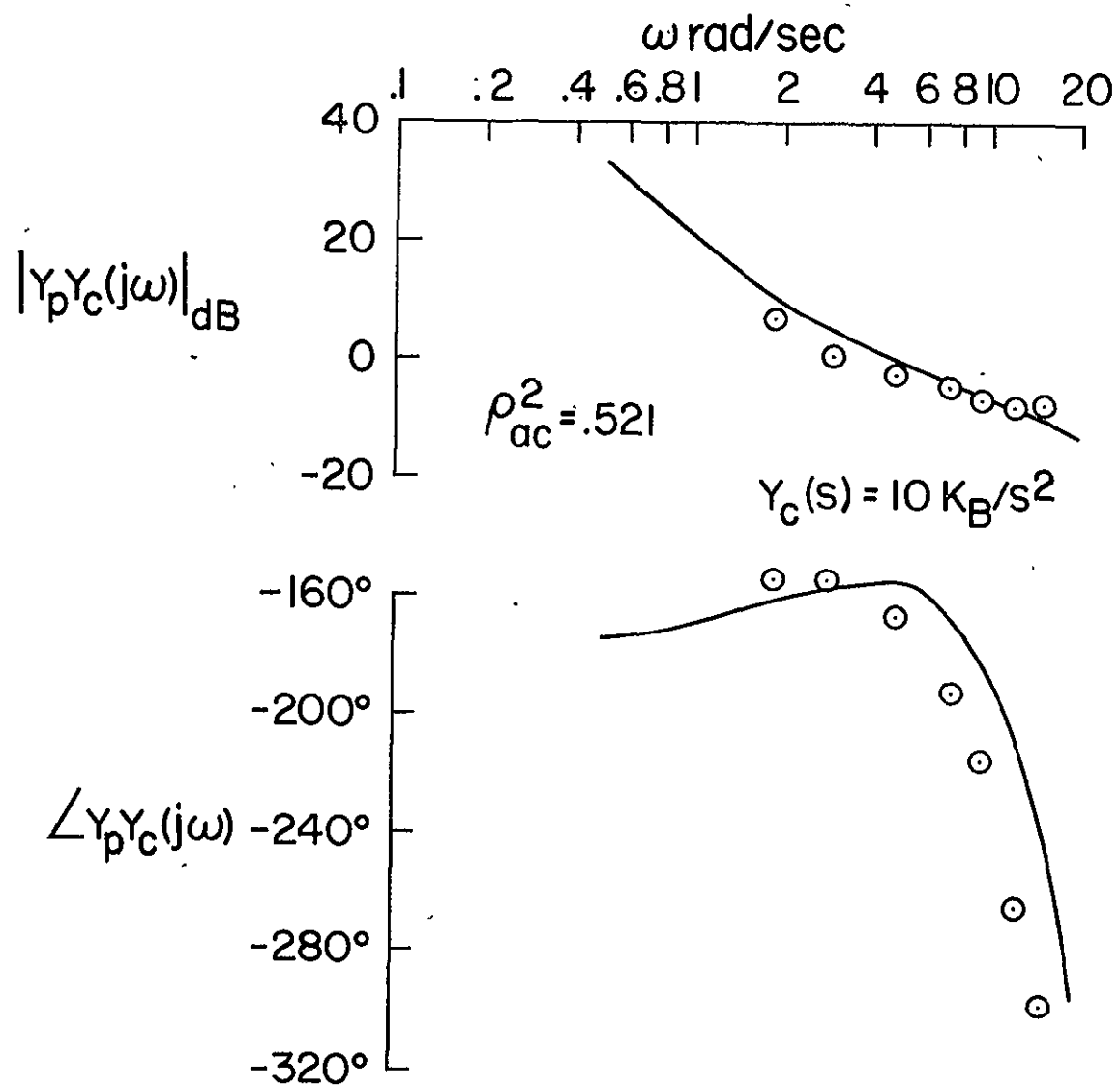


Figure 9.- A comparison of model generated and experimental open-loop describing functions for experiments from [13].

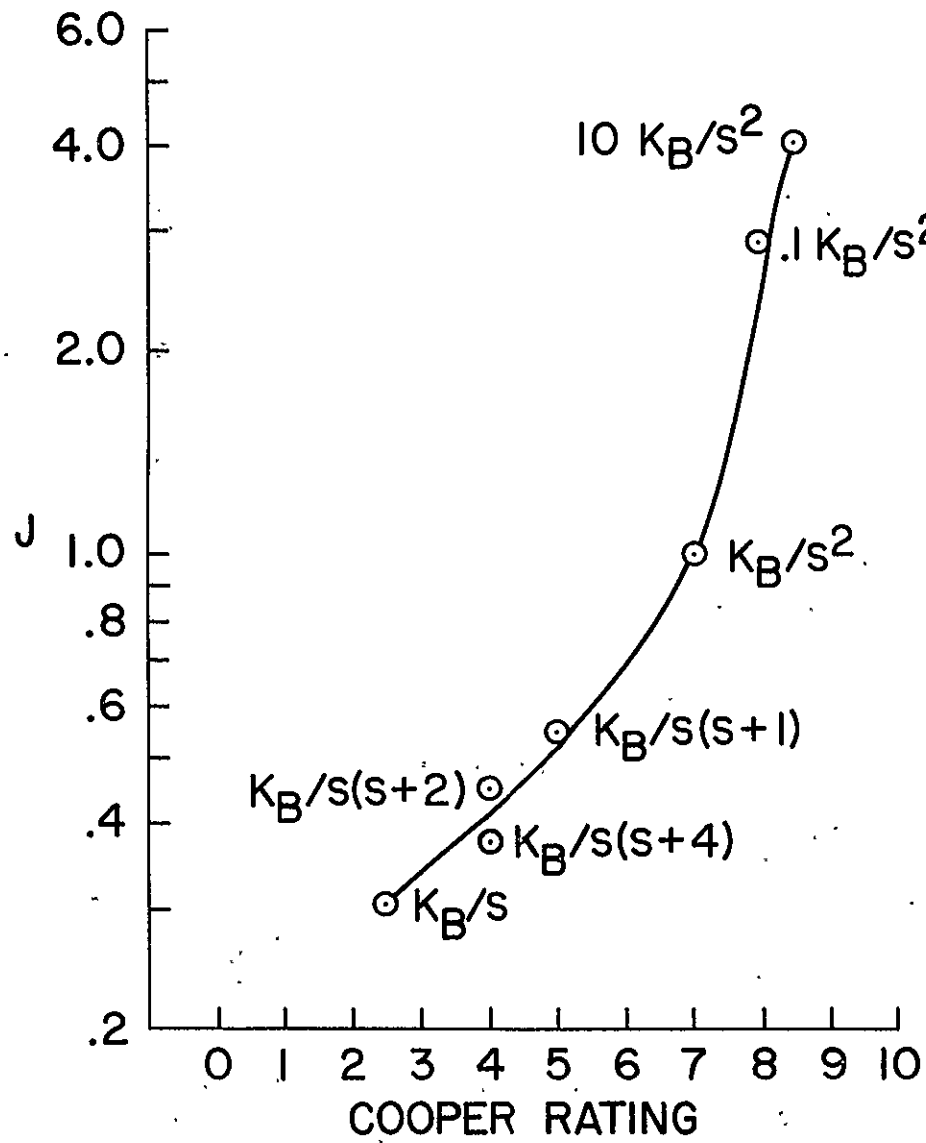


Figure 10.- Rating curve for Cooper rating scale.

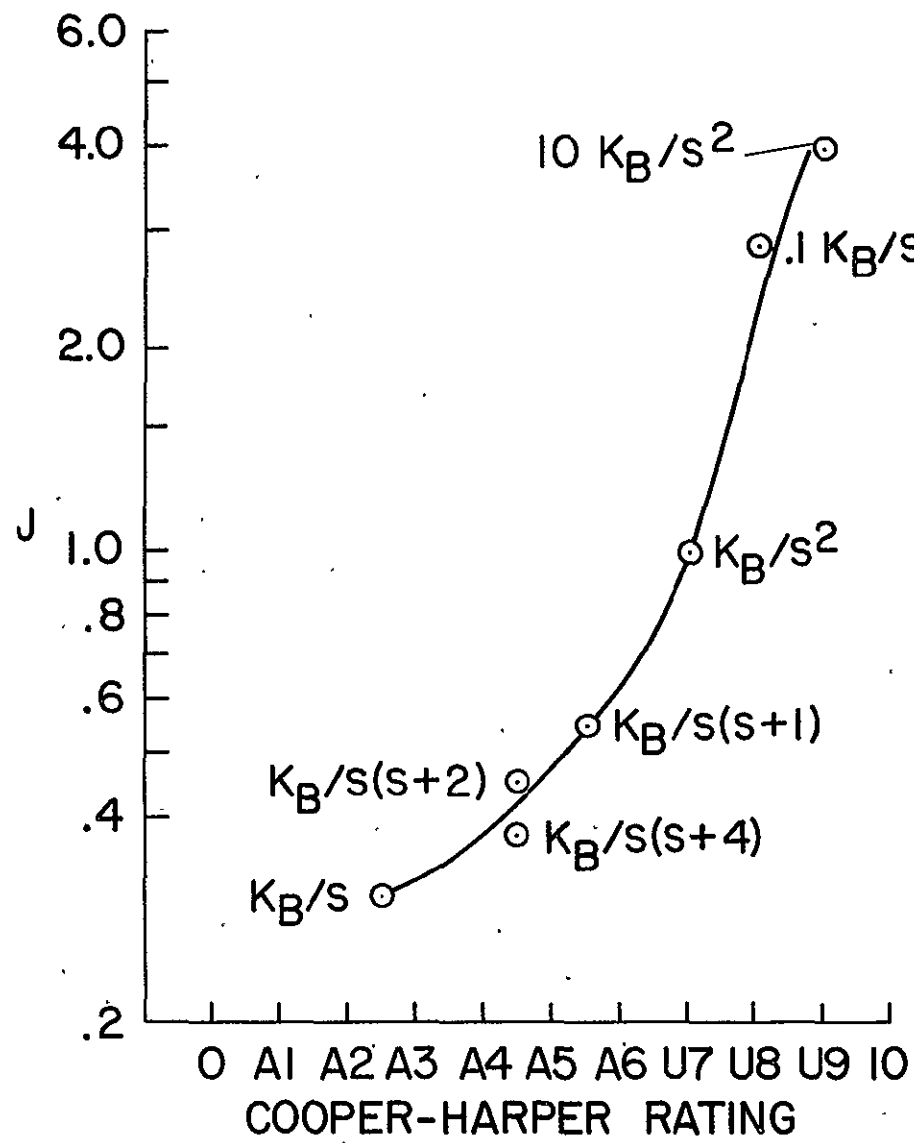
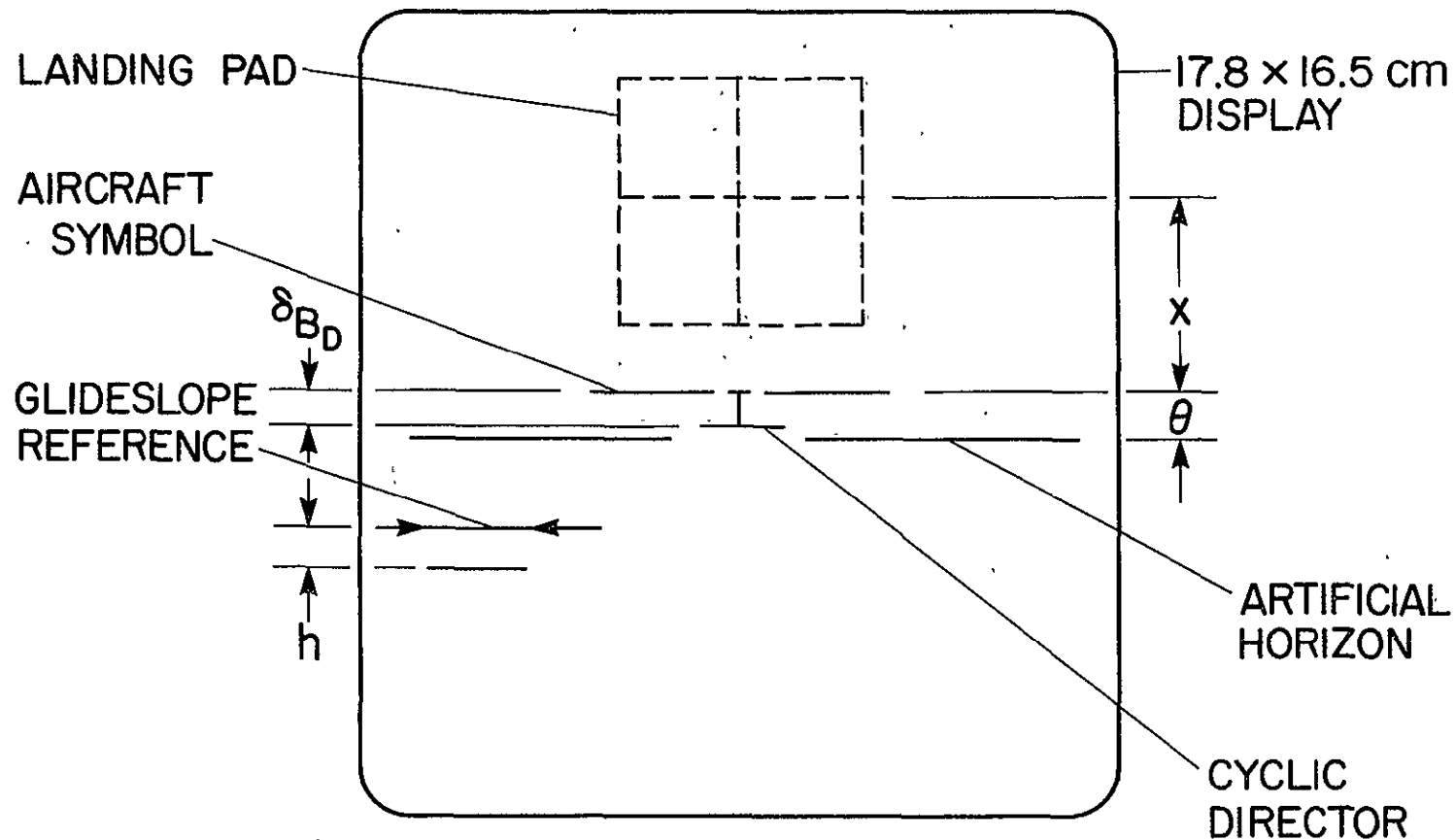


Figure 11.- Rating curve for Cooper-Harper rating scale.



DISPLAY GAINS

PITCH ATTITUDE 7.87 deg/cm
 GLIDESLOPE DEVIATION 6 m/cm
 LONGITUDINAL DISPLACEMENT 3 m/cm
 FROM LANDING PAD

Figure 12.- CRT display for UH-1H Hover.

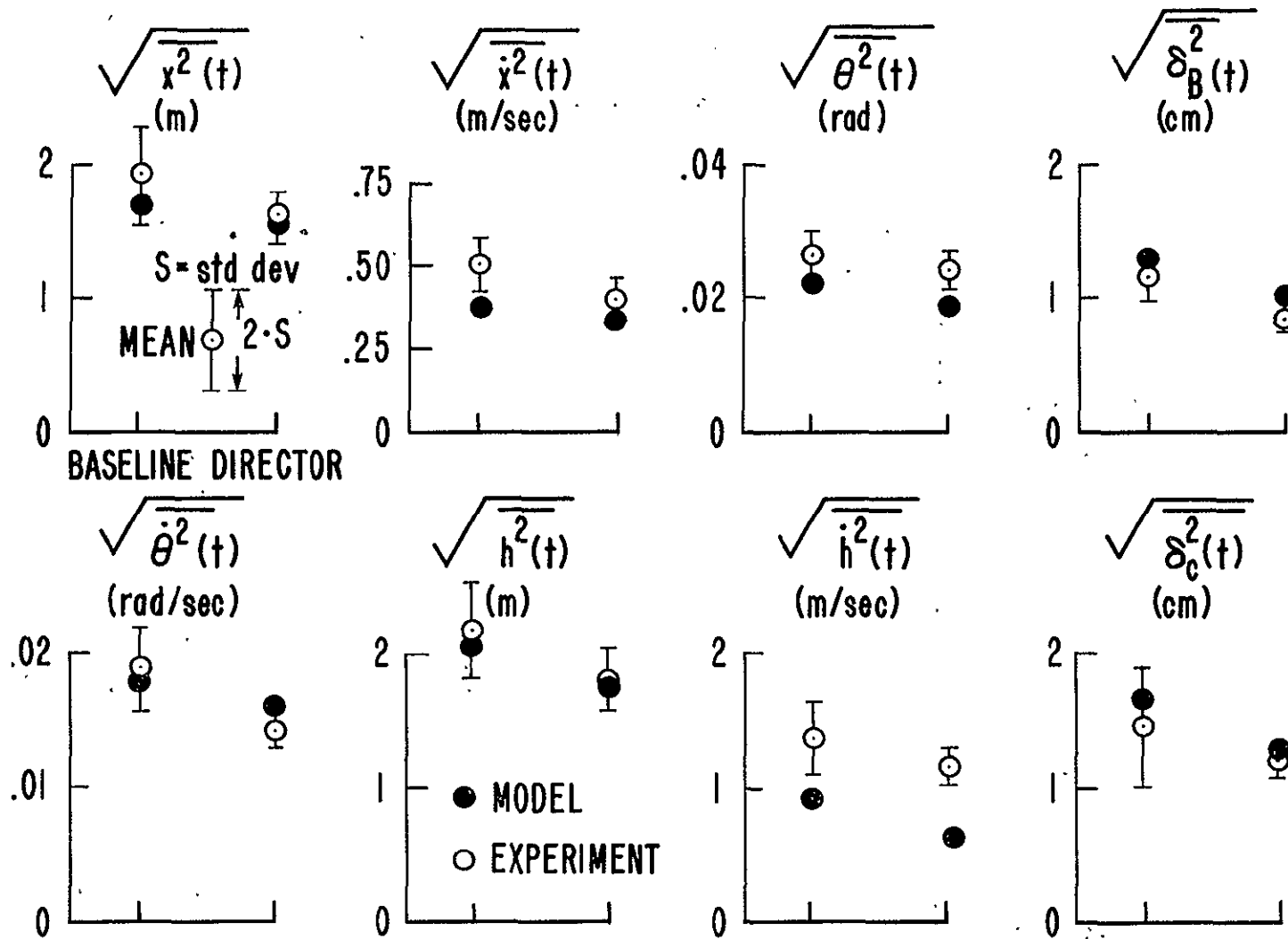
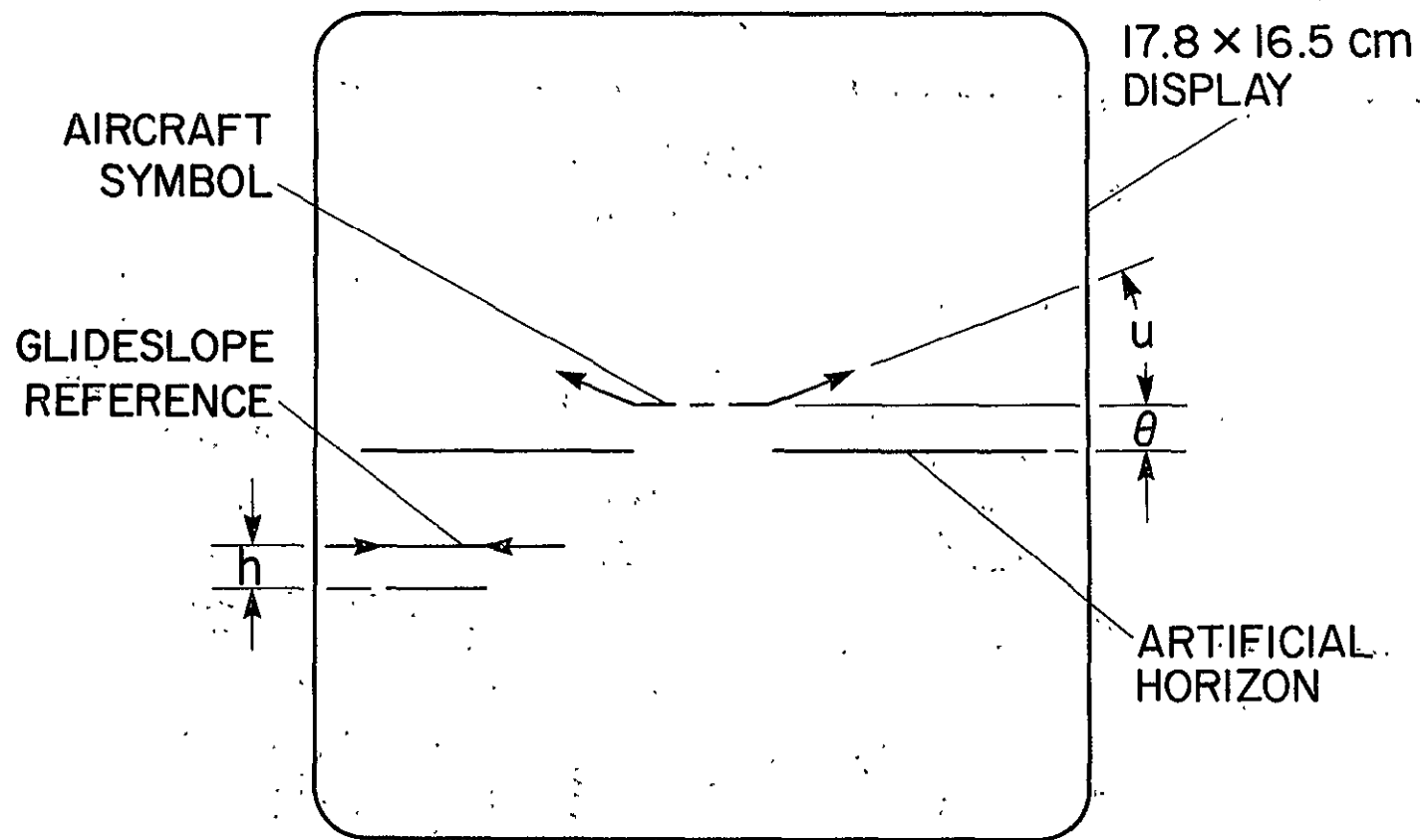


Figure 13.- Comparison of model generated and experimental tracking errors for UH-1H Hover.



DISPLAY GAINS

PITCH ATTITUDE 7.87 deg/cm

GLIDESLOPE DEVIATION 6 m/cm

GROUNDSPEED DEVIATION .257 m/sec-deg

Figure 14.- CRT display for UH-1H landing approach.

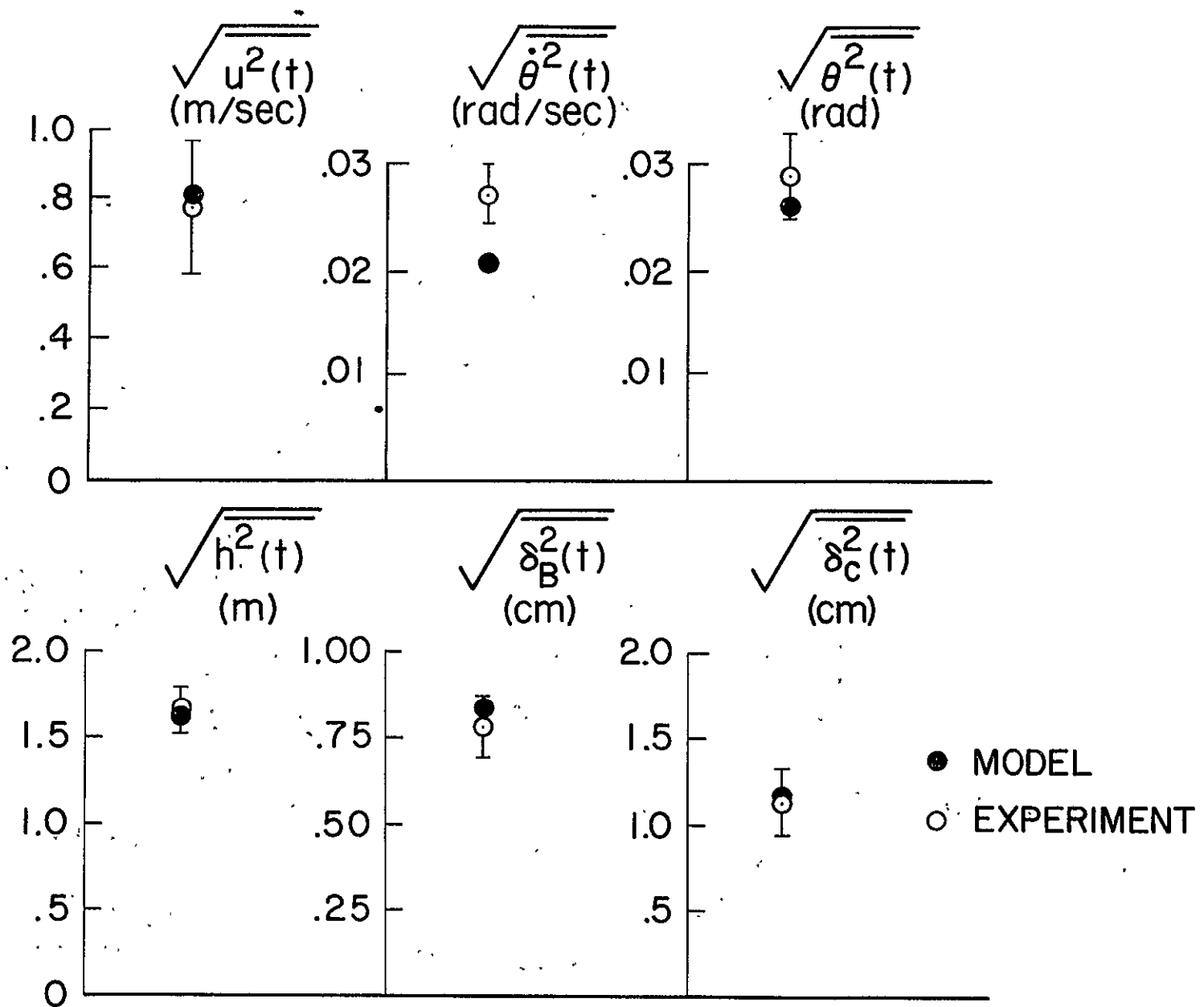
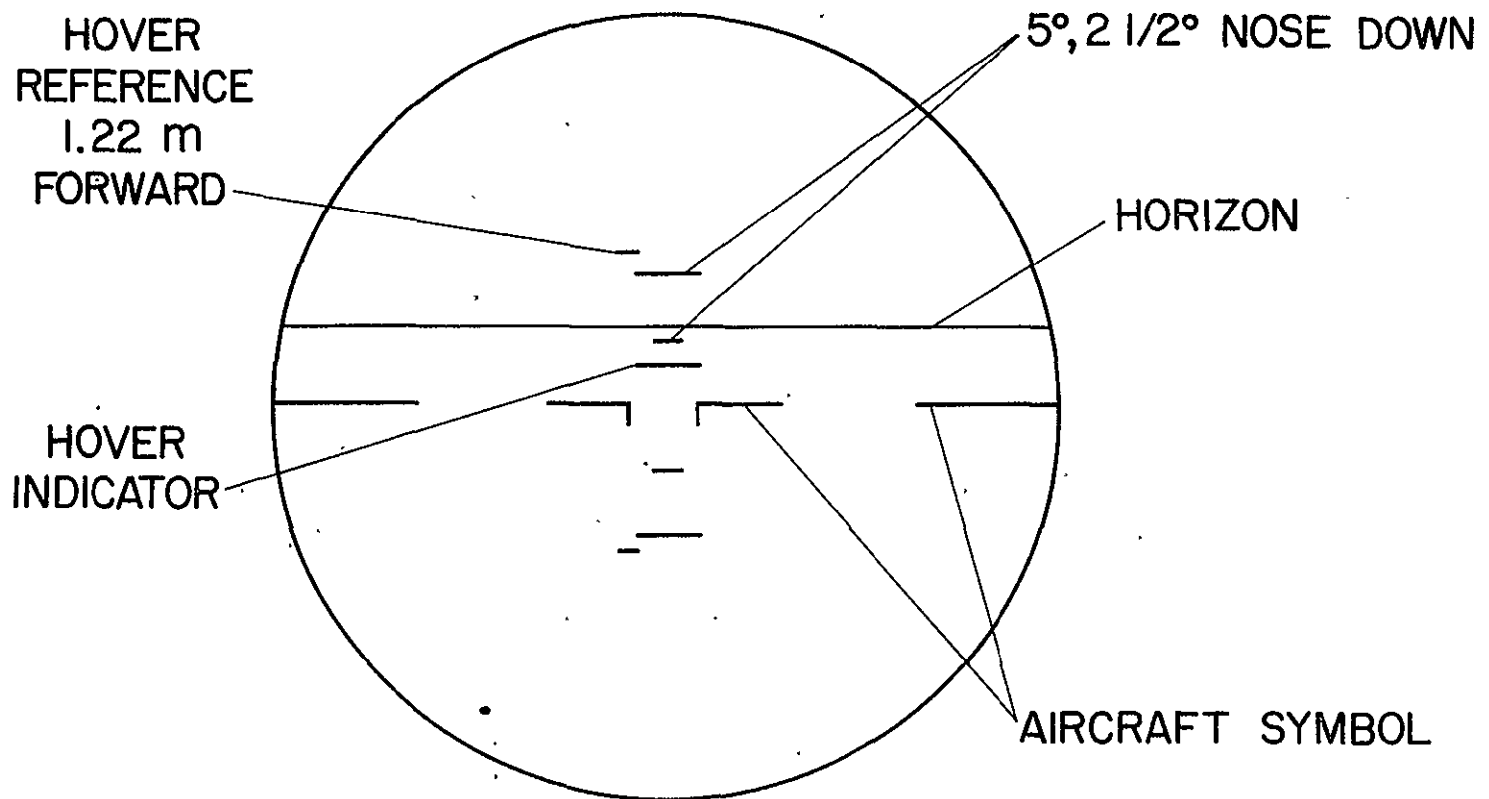


Figure 15.- Comparison of model generated and experimental tracking errors for UH-1H landing approach.



DISPLAY GAINS

PITCH ATTITUDE 2.31 deg/cm :

LONGITUDINAL DISPLACEMENT
 .542 m/cm FROM PAD CENTER

Figure 16.- CRT display for H-19 Hover.

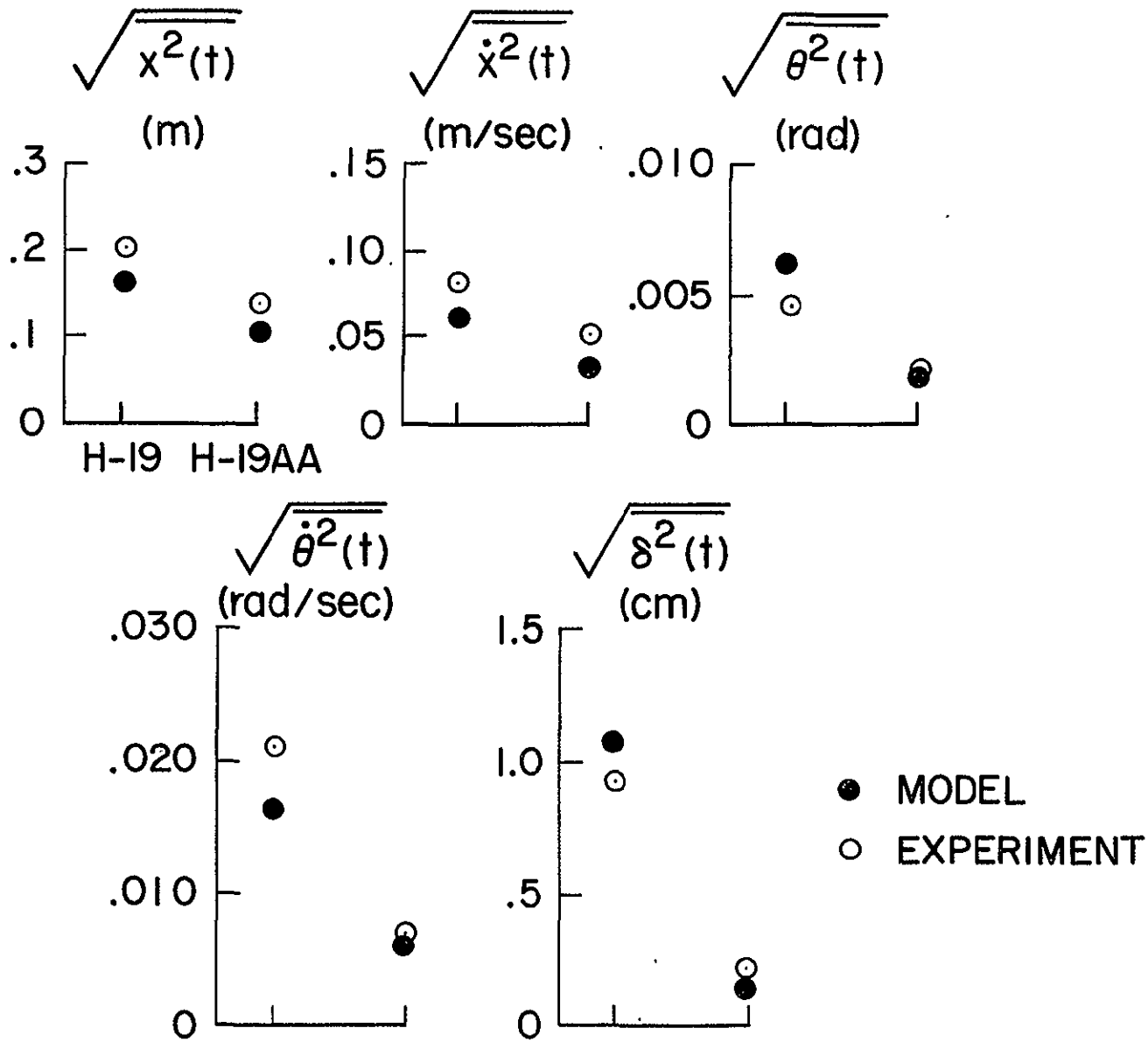


Figure 17.- Comparison of model generated and experimental tracking errors for H-19 Hover.